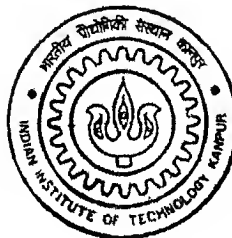


Solution of Interface/Crack Problems Using Distributed Dislocations

by
Mukesh Kumar Tripathi

TH
ME/2001/M
T 737/2



**DEPARTMENT OF MECHANICAL ENGINEERING
INDIAN INSTITUTE OF TECHNOLOGY, KANPUR**

**Solution of Interface/Crack Problems
Using Distributed Dislocations**

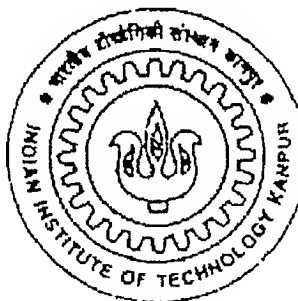
A Thesis Submitted

in partial fulfillment of the requirements

for the degree of

**Master of Technology
in
Mechanical Engineering**

**By
Mukesh Kumar Tripathi**



**Department of Mechanical Engineering
Indian Institute of Technology
Kanpur
January 2001**

$\{x_i\} \in \mathbb{R}^{n \times 1} \quad i = 1, \dots, n \}$ / M.E

2. $\bar{\epsilon}_u = 1.748$

શાસ્ત્રીય વિદ્યા

133622

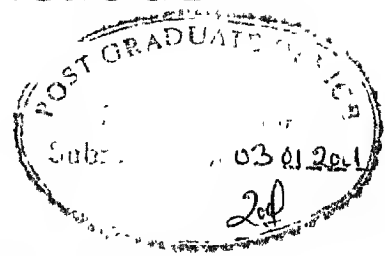
1

14220



A133622

INDIAN INSTITUTE OF TECHNOLOGY
KANPUR



Department of Mechanical Engineering

CERTIFICATE

This is to certify that Mr. Mukesh Kumar Tripathi (Roll No 9910521), a student of M.Tech. (Solid Mechanics & Design) has completed his thesis entitled "Solution of Interface/crack Problems Using Distributed Dislocations" for partial fulfillment of the degree of Master of Technology at IIT, Kanpur.



V. B. Shenoy

(Asstt. Professor)

Dept. of Mechanical Engineering

IIT Kanpur

208016

ACKNOWLEDGEMENTS

I wish to express my deep sense of gratitude and indebtedness to prof Vijay Shenoy for his invaluable guidance, constructive suggestions and detailed instructions through this work inspite of his hectic schedule

I would like to express my humble thanks to one and all who directly or indirectly helped me in completing this work

Finally I am greatful to the Almighty for what I am today.

ABSTRACT

Crack problems can be solved by using the *Distributed Dislocation Technique*, where under a given loading conditions a crack is modeled as an array of dislocations since the crack faces remain traction free, hence making use of this condition an integral equation is developed which is singular in nature. solving this integral equation with the help of *quadrature rule* we compute the dislocation density at the ends of crack tip, which in turn is used to compute the *stress intensity factor* at the tip of a crack.

After the above analysis this technique is applied to the case of *Bi-periodic cracks in an infinite body*. Results of this analysis are presented with the help of graphs.

Problem of a inclusion-interface-matrix is also solved by using the same method, here a circular inclusion, of a given radius is considered, which is subjected to uniform pressure.

Results obtained by distributed dislocation technique are also compared with the analytical results

Contents

List of Selected Symbols	vii
1 Introduction	2
1.1 Introduction	2
1.2 Fundamentals of Distributed Dislocation Technique	5
1.3 Plan of the Thesis	6
2 Dislocation Techniques	9
2.1 Stress Fields	9
2.1.1 Stress field of a dislocation with burgers vector in x-direction	9
2.1.2 Stress field of dislocation with burgers vector in y-direction.	10
2.1.3 Stress Field because of a unit dislocation lying on the boundary of a circular inclusion	10
2.2 Dislocation Density	11
2.3 Stress Intensity Factor (SIF):	12
2.4 Singular Integral Equation and Gauss-Chebyshev Quadrature	12
2.5 The Mode-I crack :	13
2.5.1 Solution using Dislocations:	13
2.5.2 Analytical result:	15
2.5.3 Comparison between Computational and Analytical Results	15
2.6 The Mode-II crack :	16
2.6.1 Solution using Dislocations:	16
2.6.2 Analytical Result	18
2.6.3 Comparison between Analytical and Computational Results	18
2.7 Arc shaped crack :	18
2.7.1 Solution using Dislocation:	18
2.7.2 Analytical Result:	21

2.7.3 Comparison between Computational and Analytical results	21
3 Complex geometries	23
3.1 Bi-Periodic cracks.	23
3.1.1 Array of cracks with periodicity Alpha in X-direction.	24
3.1.2 Array of cracks with periodicity Beta in Y-direction	24
3.2 Circular inclusion with interface	24
3.2.1 Interface Law	26
3.2.2 Problem Formulation	27
3.2.3 Analytical Result	31
3.2.4 Comparison between analytical and computational results	32
4 Conclusion and Future Scope	33
references	35

List of Selected Symbols

a	Crack length,one half of total length of internal crack
b_x	Component of burger's vector in x-direction
b_y	Component of burger's vector in y-direction
b_ρ	Component of burger's vector in radial direction
μ	Shear modulus
ν	Poisson's ratio
K_O	Nominal SIF for a crack in infinite solid
K_I	Stress intensity factor for mode-I
K_{II}	Stress intensity factor for mode-II
σ_{ij}^x	Stress tensor because of x-dislocation
σ_{ij}^y	Stress tensor because of y-dislocation
σ_{ij}^ρ	Stress tensor because of dislocation with burger's vector in radial direction
σ_{ij}^t	Stress tensor because of dislocation with burger's vector in tangential direction
ψ_x	Dislocation density of in x-direction
ψ_y	Dislocation density of in y-direction
ψ_ρ	Dislocation density of in radial direction
ψ_t	Dislocation density of in tangential direction
u_r	Jump-in-displacement in radial direction
u_t	Jump-in-displacement in tangential direction

List of Figures

1.1	Typical two- dimensional elements	3
1.2	A rectangular element mesh and path of integration for J-Integral	3
1.3	Quarter point elements around a crack tip	4
1.4	The creation of an edge dislocation.(a) by an opening displacement(climb) or (b) by a tangential displacement (glide)	6
1.5	Application of Buckner's principle:(a) overall problem (b)stress in perfect body (c) separated material	7
1.6	The Insertion of material between the crack faces by adding and taking away thin strips	8
2.1	(a), (b) are Dislocations with Burgers vector in x and y direction respectively	9
2.2	A dislocation on the boundary of a circular inclusion	10
2.3	Mode-I crack subjected to far field P	14
2.4	Mode-II crack subjected to far field P	16
2.5	Arc shaped crack subjected to uniform pressure	19
2.6	Rotation Matrix	20
2.7	Graph Showing the variation of K_{II} vs N :	22
2.8	Graph Showing the variation of SIF vs 2α :	22
3.1	Bi periodic cracks in an infinite body with periodicity alpha in x-direction and Beta in Y-direction:	23
3.2	Array of cracks in an infinite body with periodicity α in x-direction where $\beta >> \alpha$	24
3.3	Graphs showing the variation of K_I/K_0 vs periodicity in x direction i.e. Alpha for different values of beta	25
3.4	Graphs showing the variation of K_{II}/K_0 vs periodicity in x direction i.e. Alpha for different values of beta	25
3.5	Array of cracks in an infinite body with periodicity beta in y-direction	26

3 6	Graphs showing the variation of KI/KO vs periodicity in y direction i.e Beta for different values of Alpha	27
3 7	A circular inclusion subjected to uniform far field pressure σ	28
3 8	Rotation Matrix	30

Chapter 1

Introduction

1.1 Introduction

Finite Element Method (FEM) is one of the numerical methods to obtain an approximate solution of the engineering problems. Applications include structures, solid mechanics, heat conduction, vibrations, elasto-plastic analysis, fluid flow etc. Finite element method is widely used in fracture mechanics applications. In FEM the domain of the problem is discretized into a number of subdomains, called finite elements, connected with one another at points known as nodes. The variables of the problem, such as displacements, temperature, velocity, etc., are approximated piecewise, so that they are represented in each element by simple polynomials. The coefficients of the polynomials are determined such that the governing equation and boundary conditions are satisfied in a best possible manner. The solution becomes more and more accurate by choosing smaller elements and more number of nodal variables. The necessary and sufficient conditions on the nodal variables and the shape functions to assure the convergence are well laid out in FEM theory. Some of the typical two dimensional elements used to discretize the domain are shown in the figure.

Two-dimensional problems of fracture mechanics are solved through FEM, in general, by using the triangular, quadrilateral or isoparametric elements. However there are certain limitations of the simple elements to represent large stress gradients. The stress gradient near the crack tip is very high, and theoretically, stress becomes singular at the crack tip. To represent such large stresses and stress gradients reasonably well, we need to employ very fine mesh near the crack tip. This involves large amount of computational complexity.

Computed value of SIF has an error of 11% with coarse mesh and 5% when a very fine mesh is used.

There are several indirect methods which do take care of high stress gradient near the crack

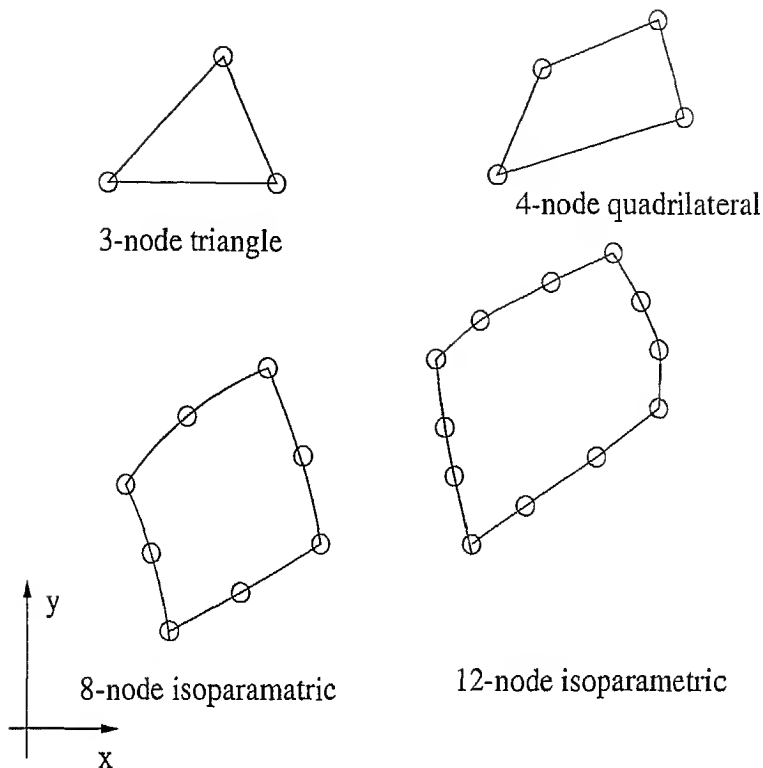


Figure 1.1. Typical two- dimensional elements

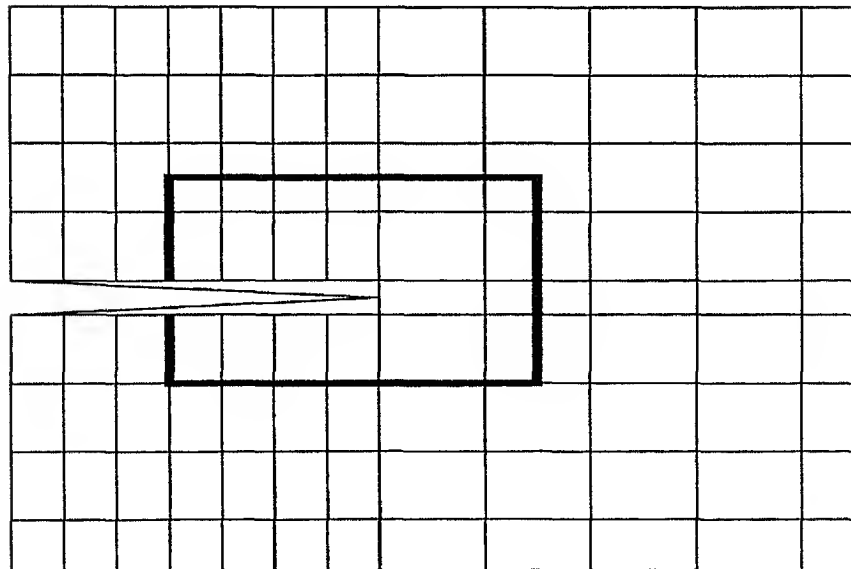
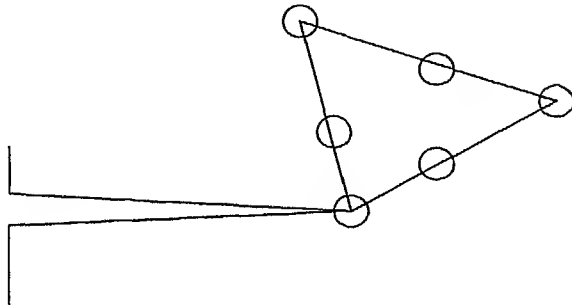


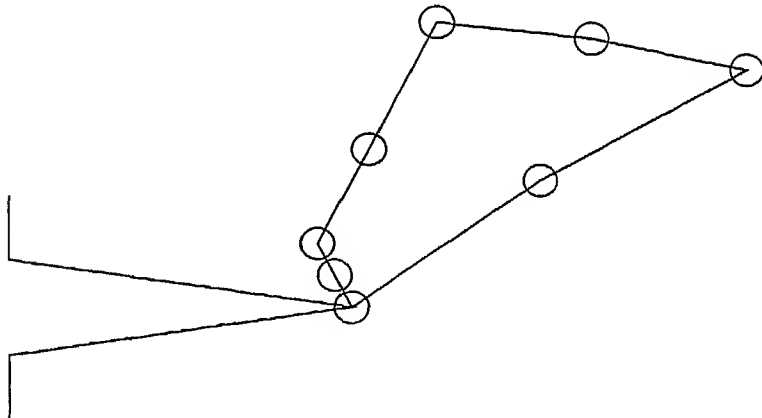
Figure 1.2: A rectangular element mesh and path of integration for J-Integral

tip. They make use of some knowledge of crack behaviour in finite element analysis which will markedly improve the accuracy of the results. The most popular method is the J- Integral method. In this method a path is chosen from one crack surface to the other crack surface thus

surrounding the crack tip. This integral value can be evaluated on a path which is slightly away from the crack tip. The resulting stress intensity factor is quite accurate having an error of 3.5%. Another method is by employing the energy release rate technique. This involves the evaluation of energy in the cracked body for two slightly different configurations. The energy release rate G can be written in terms of SIF . This computed SIF has an error of 3%



Triangular element



Quadrilateral element

Figure 1.3: Quarter point elements around a crack tip

Another simulation of singularity is by the use of quarter point element technique. In this technique usual isoparametric 6-noded triangle or 8-noded isoparametric quadrilateral elements are employed. Midside nodes on the two adjacent side are shifted towards the corner node to the quarter point locations. For these locations of the mid nodes the stresses becomes singular. In the figure observe that all the midside nodes adjacent to the crack tip are at quarter point location. It has been demonstrated that SIF found by this method is within 2% of the theoretical solutions.

The technique presented in this thesis is based on the pioneering work of Eshelby in the late

1950's, and developed by Erdogan, Keer and Mura. The basic idea of this technique is to use the superposition of the stress field present in the unflawed body, together with an unknown distribution of 'strain nuclei'(Dislocations), chosen so that the crack faces become traction-free. The solution used for the stress field for the nucleus is chosen so that other boundary conditions are satisfied. The technique is therefore efficient, and may be used to model the evolution of a developing crack in two or three dimensions.

The basic strategy used is to cancel the unwanted tractions appearing along the faces of flaws by distributing various kinds of strain nuclei(Dislocations) along the length of flaw in two dimension. Dislocations are the point source of strain (or stress). The problem is solved in three parts. first the stress in the body are found in the absence of the flaw, by any suitable method, the stress due to the chosen kind of strain nucleus are found, in the same geometry, any number of strain nuclei may be distributed through the body without violating the surface boundary conditions. The problem therefore remains only to distribute the strain nuclei in such a way as to ensure that the crack faces remain traction free, and in order to do this an *Integral Equation* is established which typically must be solved by an appropriate numerical quadrature, this constitute the third part of the problem

In two dimension, a *dislocation* may be created by first making a slit in an solid, the trajectory of slit may take any form, and the dislocation is formed by imposing a constant displacement between adjacent points located either side of slit, by inserting or removing the material as necessary, and then welding the material back together, the constant relative displacement imposed is known as *Burgers Vector*.

The jargon 'climb' and 'glide' dislocation is defined as follows: If the Burgers Vector is *Perpendicular* to the path cut, so that a strip is inserted as shown in figure (1.4), the dislocation is said to be 'climb'. If the Burgers Vector is *parallel* to the path cut, so that there are shear displacement, the dislocation is said to be 'glide', and the path cut defines the 'glide plane'.

1.2 Fundamentals of Distributed Dislocation Technique

In order to introduce the technique in the simplest possible way consider a *plane* problem. fig(1.5) shows a plane crack opened by a tensile field. From Buckner's theorem [ref-12] the solution to this problem can be obtained by a superposition of the problems as shown in the figure. These are the stresses arising in the uncracked body, and the stresses induced in the *unloaded* body, due to application of equal and opposite traction to those present along the line of the crack in the problem. The strategy adopted to generate the *corrective* traction as shown in the figure is to make a fine slit along the line of the crack; the two sides of the cut are then separated by inserting

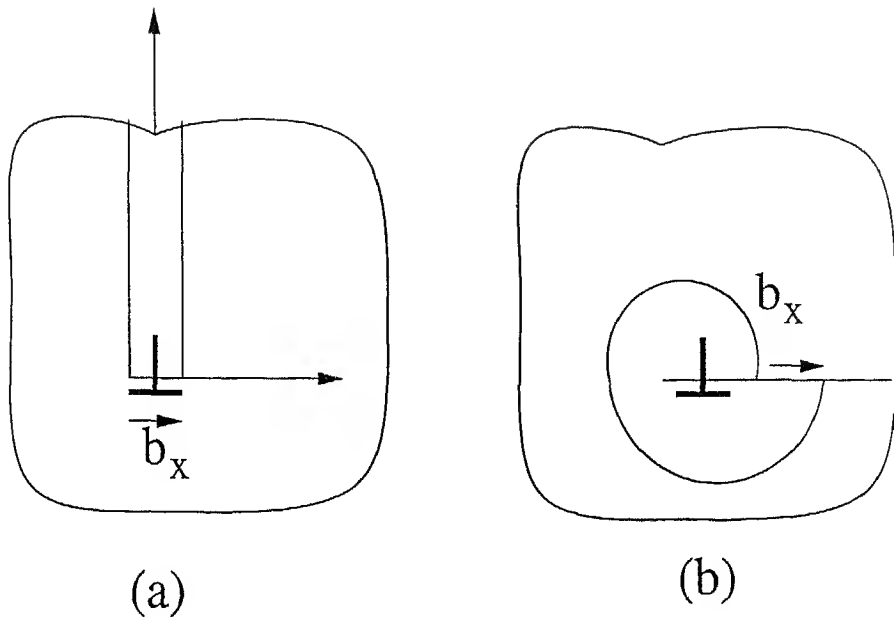


Figure 1.4: The creation of an edge dislocation.(a) by an opening displacement(climb) or (b) by a tangential displacement (glide)

material to fill ‘the crack’ as shown, the interior of the real open crack is, of course, empty; the inserted material is simply a mathematical device-a means of generating the corrective traction, and at the same time simulating separation of the crack-faces.

It is helpful to visualize the inserted material as a combination of infinitesimally thin strips, the first begining at one crack-end and extending to infinity, or a remote boundary,as shown in the figure(1.5); more strips are added as shown in the figure and, finally, strips of material are taken away so that the geometries of figure(1.6) are recovered. The stress field due to the complete array of strips may be obtained by a simple addition, or integration, of the solutions for single strips.

The single inserted thin strip of material is the familiar *edge* dislocation, so that the strain nucleus appropriate to plane crack problems, and which we will employ throughout this report, is the straight dislocation.

1.3 Plan of the Thesis

The second chapter of this thesis covers the ModeI, Mode-II, problems of a straight and an arc shaped crack. Results obtained with the *Distributed Dislocation Technique* and the results

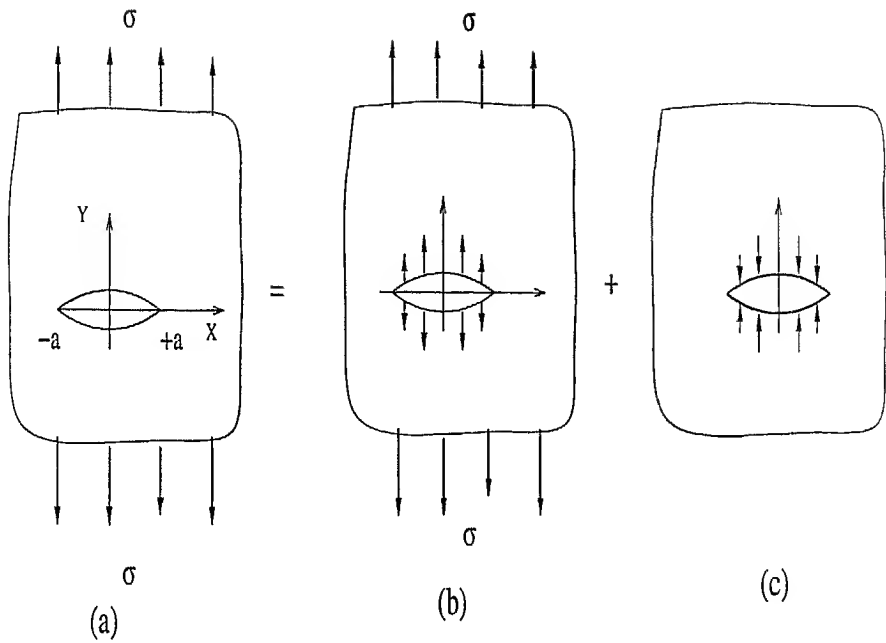


Figure 1.5: Application of Buckner's principle (a) overall problem (b) stress in perfect body (c) separated material

available in the literature are given in this chapter. This chapter actually proves the validity of *Distributed Dislocation Technique*. Definitions of some basic terms e.g. SIF, Dislocation Density etc. are also given in this chapter. Method of handling a *singular integral equation* is also discussed in this chapter.

Third chapter of this report covers some more complex cases. This chapter covers the problem of bi-periodic cracks in a body. effect of *periodicity* on the SIF is presented with the help of graphs. Last part of this chapter covers a circular inclusion problem subjected to uniform pressure.

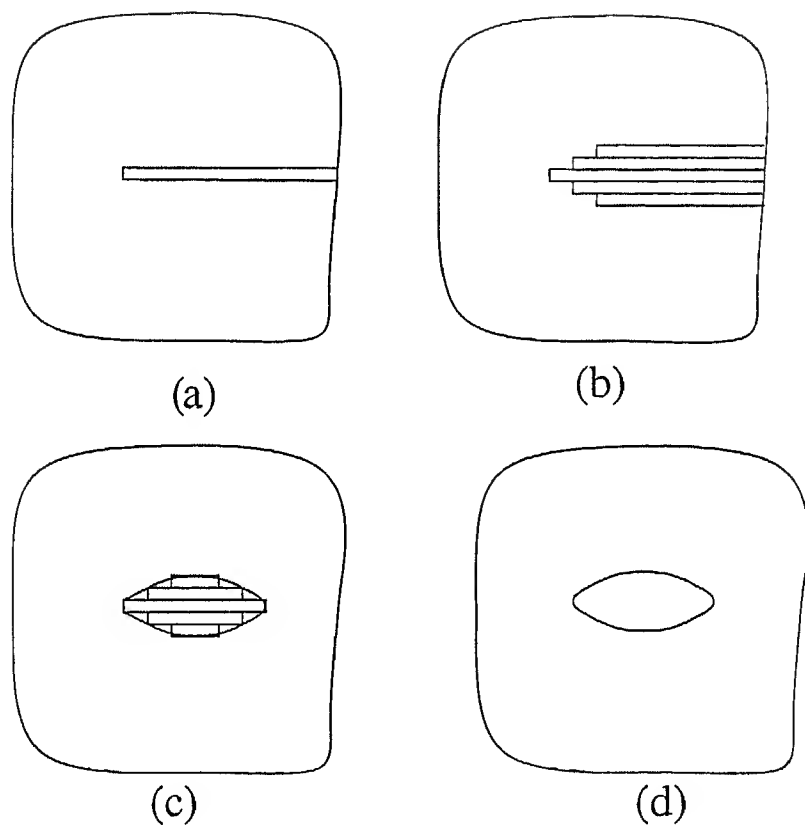


Figure 1.6: The Insertion of material between the crack faces by adding and taking away thin strips

Chapter 2

Dislocation Techniques

2.1 Stress Fields

The stress field of a dislocation located at the origin in a material whose elastic properties are μ and ν , where b is the burgers vector of the dislocation.

2.1.1 Stress field of a dislocation with burgers vector in x-direction:

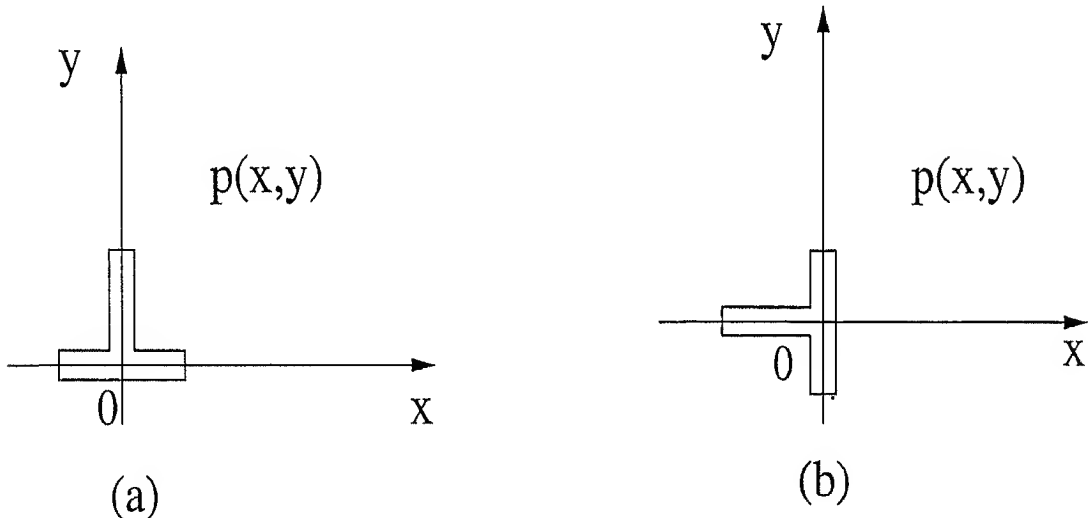


Figure 2.1: (a), (b) are Dislocations with Burgers vector in x and y direction respectively

$$\sigma_{xx} = \frac{-\mu b}{2\pi(1-\nu)} \frac{y(3x^2 + y^2)}{(x^2 + y^2)^2} \quad (2.1)$$

$$\sigma_{yy} = \frac{\mu b}{2\pi(1-\nu)} \frac{y(x^2 - y^2)}{(x^2 + y^2)^2} \quad (2.2)$$

$$\sigma_{xy} = \frac{\mu b}{2\pi(1-\nu)} \frac{x(x^2 - y^2)}{(x^2 + y^2)^2} \quad (2.3)$$

2.1.2 Stress field of dislocation with burgers vector in y-direction:

$$\sigma_{xx} = \frac{\mu b}{2\pi(1-\nu)} \frac{x(x^2 - y^2)}{(x^2 + y^2)^2} \quad (2.4)$$

$$\sigma_{yy} = \frac{\mu b}{2\pi(1-\nu)} \frac{x(3y^2 + x^2)}{(x^2 + y^2)^2} \quad (2.5)$$

$$\sigma_{xy} = \frac{\mu b}{2\pi(1-\nu)} \frac{y(x^2 - y^2)}{(x^2 + y^2)^2} \quad (2.6)$$

2.1.3 Stress Field because of a unit dislocation lying on the boundary of a circular inclusion

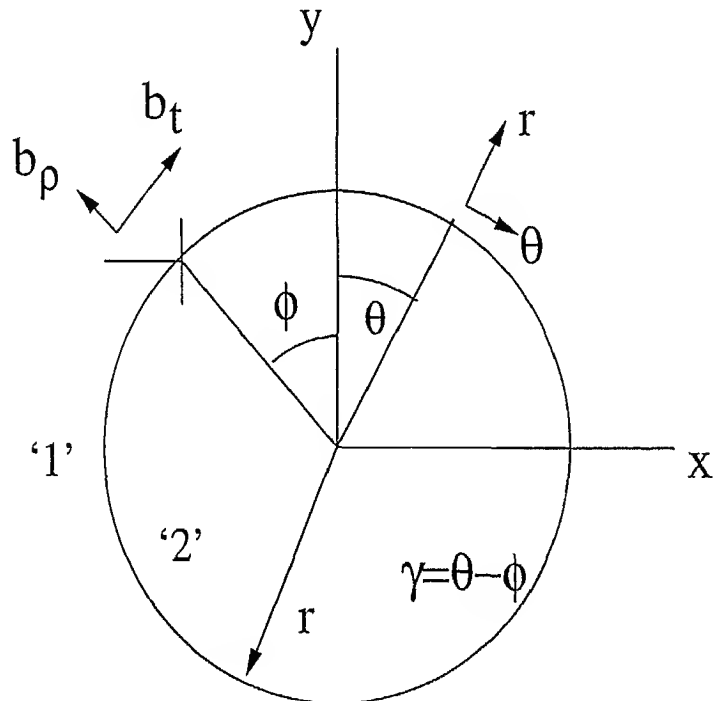


Figure 2.2: A dislocation on the boundary of a circular inclusion

$$\sigma_{rr}^p = \frac{C}{\pi} \left[\frac{\beta \sin \gamma}{2r} + \frac{\sin \gamma \cos \gamma}{2r(1 - \cos \gamma)} \right] \quad (2.7)$$

$$\sigma_{r\theta}^{\rho} = \frac{C}{2r\pi} [\beta - (1 - \beta) \cos \gamma] \quad (2.8)$$

$$\sigma_{rr}^t = \frac{C}{2r\pi} \left[\frac{2 - \beta(1 + \alpha)}{1 + \alpha - 2\beta} + (1 - \beta) \cos \gamma \right] \quad (2.9)$$

$$\sigma_{r\theta}^t = \frac{C}{\pi} \left[\frac{\beta \sin \gamma}{2r} + \frac{\sin \gamma \cos \gamma}{2r(1 - \cos \gamma)} \right] \quad (2.10)$$

where,

$$C = \frac{2\mu_1(1 + \alpha)}{(\kappa_1 + 1)(1 - \beta^2)} = \frac{2\mu_2(1 - \alpha)}{(\kappa_2 + 1)(1 - \beta^2)} \quad (2.11)$$

μ_1, ν_1 and μ_2, ν_2 are modulus of rigidity and Poisson's ratio of the material '1' and '2'. α and β are the Dundurs parameters given by

$$\alpha = \frac{\mu_2(\kappa_1 + 1) - \mu_1(\kappa_2 + 1)}{\mu_2(\kappa_1 + 1) + \mu_1(\kappa_2 + 1)}$$

$$\beta = \frac{\mu_2(\kappa_1 - 1) - \mu_1(\kappa_2 - 1)}{\mu_2(\kappa_1 + 1) + \mu_1(\kappa_2 + 1)}$$

κ is the Kolosov's constant: $\kappa = 3 - 4\nu$

superscript 'ρ' and 't' indicates the stress field because of dislocation with burgers vector in radial and tangential direction respectively.

2.2 Dislocation Density

The *Dislocation Density* physically represents the negative of the slope at any point between the crack faces. Thus if $g(x)$ represents the amount of opening from the end of a crack then,

$$g(x) = - \int_{-a}^x \psi(\xi) d\xi \quad (2.12)$$

or,

$$\psi(\xi) = - \frac{dg(\xi)}{d\xi} \quad (2.13)$$

where $\psi(\xi)$ represents the dislocation density at the point ξ . Note that, since the opening displacement is parabolic in form near the crack tips, the density must tend to infinity in a *Square root singular* manner as the crack tip is approached.

2.3 Stress Intensity Factor (SIF):

The Stress intensity factor denoted by K is a measure of the stress singularity at a crack tip. This stress singularity is square root dependent with the distance from the crack tip. If the magnitude of K at a tip is known for a crack which is subjected to a given stress field then K remains a measure of how close the crack is to a fracture condition.

SIF can be computed from the dislocation function density by the following formula:

$$K_{II} + iK_I = \frac{\mu}{2(1-\nu)} \lim_{x \rightarrow a} \sqrt{2\pi(a-x)} [\psi_x(x) + i\psi_y(x)] \quad (2.14)$$

In terms of non dimensional parameter SIF is given as

$$K_{II} + iK_I = \frac{\mu}{2(1-\nu)} \lim_{\eta \rightarrow 1} \sqrt{2\pi(1-\eta)} [\psi_x(\eta) + i\psi_y(\eta)] \quad (2.15)$$

where K_I : Stress Intensity factor for Mode-I condition

K_{II} : Stress Intensity factor for Mode-II condition

ψ_x and ψ_y are the dislocation densities for x and y dislocations respectively.

2.4 Singular Integral Equation and Gauss-Chebyshev Quadrature

Consider the following singular integral :

$$S(x) = \frac{1}{\pi} \int_{-1}^{+1} \frac{\psi(t)dt}{t-x}, -1 < x < 1 \quad (2.16)$$

where

$$\psi(t) = R(t)F(t), \text{ and } R(t) = \sqrt{1-t^2}$$

let us assume that $F(t)$ can be approximated to a sufficient degree of accuracy by the following truncated series :

$$F(t) \approx \sum_{i=0}^n a_i T_i(t)$$

so now the integral equation becomes

$$S(x) \approx \sum_{i=0}^n a_i \frac{1}{\pi} \int_{-1}^{+1} \frac{T_i(t)dt}{(t-x)\sqrt{1-t^2}} = \sum_{i=1}^n a_i U_{i-1}(x) \quad (2.17)$$

where the following relation is used :

$$\frac{1}{\pi} \int_{-1}^{+1} \frac{T_i(t)dt}{(t-x)\sqrt{1-t^2}} = \begin{cases} U_{i-1}(x), & \text{for } i > 0 \\ 0 & \text{for } i = 0 \end{cases}$$

now for $x = x_k$

$$S(x_k) \approx \sum_{i=1}^n a_i U_{i-1}(x_k) \quad (2.18)$$

but for $0 < i < n$

$$U_{i-1}(x_k) = \sum_{j=1}^n \frac{T_i(t_j)}{n(t_j - x_k)}$$

and $T_n(t_j) = 0$, $U_{n-1}(x_k) = 0$

where $T_n(x)$ and $U_n(x)$ are chebyshev polynomials defined by

$$T_n(x) = \cos(n\theta), \quad U_n(x) = \frac{\sin(n+1)\theta}{\sin\theta}, \quad \cos(\theta) = x \quad (2.19)$$

so our singular integral equation now can be represented in the form of a sum computed at x_k points and is given by

$$S(x_k) = \sum_{i=1}^n \sum_{j=1}^n \frac{a_i T_i(t_j)}{n(t_j - x_k)} \quad (2.20)$$

where

$$\begin{aligned} T_n(t_j) &= 0, & t_j &= \cos(\pi(2j-1)/2n), & j &= 1, \dots, n \\ U_{n-1}(x_k) &= 0, & x_k &= \cos(k\pi/n), & k &= 1, \dots, n-1 \end{aligned} \quad (2.21)$$

2.5 The Mode-I crack :

2.5.1 Solution using Dislocations:

ModeI crack is shown in the fig 2.5.1. The governing integral equation is written below where we are computing the stress field at the point x because of a dislocation with unit burgers vector situated at the point x' .

$$\int_{-a}^{+a} \sigma_{yy}^x(x, x') \psi_x(x') dx' + \int_{-a}^{+a} \sigma_{yy}^y(x, x') \psi_y(x') dx' + \sigma^\infty = 0 \quad (2.22)$$

$$\int_{-a}^{+a} \sigma_{xy}^x(x, x') \psi_x(x') dx' + \int_{-a}^{+a} \sigma_{xy}^y(x, x') \psi_y(x') dx' = 0 \quad (2.23)$$

$$\psi_x(x') = \frac{g(x')}{\sqrt{(a^2 - x^2)}}, \quad \psi_y(x') = \frac{f(x')}{\sqrt{(a^2 - x^2)}} \quad (2.24)$$

rewriting the equation,

$$\int_{-a}^{+a} \sigma_{yy}^x(x, x') \frac{g(x')}{\sqrt{(a^2 - x^2)}} dx' + \int_{-a}^{+a} \sigma_{yy}^y(x, x') \frac{f(x')}{\sqrt{(a^2 - x^2)}} dx' + \sigma^\infty = 0 \quad (2.25)$$

$$\int_{-a}^{+a} \sigma_{xy}^x(x, x') \frac{g(x')}{\sqrt{(a^2 - x^2)}} dx' + \int_{-a}^{+a} \sigma_{xy}^y(x, x') \frac{f(x')}{\sqrt{(a^2 - x^2)}} dx' = 0 \quad (2.26)$$

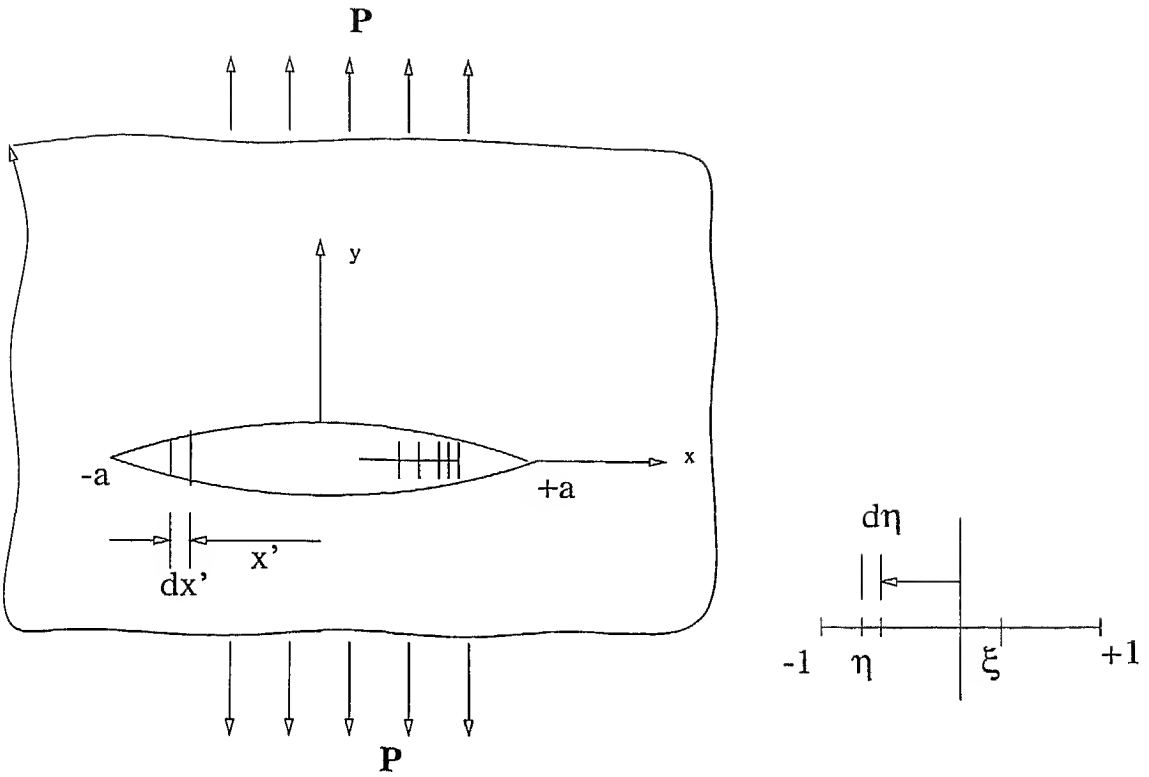


Figure 2.3: Mode-I crack subjected to far field P

writing the above equation in non dimensional terms

$$\int_{-1}^{+1} \frac{\sigma_{yy}^x(\xi, \eta)}{\sqrt{1 - \eta^2}} g(\eta) d\eta + \int_{-1}^{+1} \frac{\sigma_{yy}^y(\xi, \eta)}{\sqrt{1 - \eta^2}} f(\eta) d\eta + \sigma^\infty = 0 \quad (2.27)$$

$$\int_{-1}^{+1} \frac{\sigma_{xy}^x(\xi, \eta)}{\sqrt{1 - \eta^2}} g(\eta) d\eta + \int_{-1}^{+1} \frac{\sigma_{xy}^y(\xi, \eta)}{\sqrt{1 - \eta^2}} f(\eta) d\eta = 0 \quad (2.28)$$

expressing $g(\eta)$ and $f(\eta)$ in terms of unknown coefficient and known polynomials,

$$g(\eta) = \sum_{i=1}^n a_i T_{i-1}(\eta), \quad f(\eta) = \sum_{i=1}^n b_i T_{i-1} \quad (2.29)$$

$$\sum_{i=1}^n \left[\int_{-1}^{+1} \frac{\sigma_{yy}^x(\xi, \eta)}{\sqrt{1 - \eta^2}} T_{i-1}(\eta) d\eta \right] a_i + \sum_{i=1}^n \left[\int_{-1}^{+1} \frac{\sigma_{yy}^y(\xi, \eta)}{\sqrt{1 - \eta^2}} T_{i-1}(\eta) d\eta \right] b_i + \sigma^\infty = 0 \quad (2.30)$$

$$\sum_{i=1}^n \left[\int_{-1}^{+1} \frac{\sigma_{xy}^x(\xi, \eta)}{\sqrt{1 - \eta^2}} T_{i-1}(\eta) d\eta \right] a_i + \sum_{i=1}^n \left[\int_{-1}^{+1} \frac{\sigma_{xy}^y(\xi, \eta)}{\sqrt{1 - \eta^2}} T_{i-1}(\eta) d\eta \right] b_i = 0 \quad (2.31)$$

applying the quadrature rule

$$\sum_{i=1}^n \frac{\pi}{n} \sum_{j=1}^n [\sigma_{yy}^x(\xi_k, \eta_j) T_{i-1}(\eta_j)] a_i + \sum_{i=1}^n \frac{\pi}{n} \sum_{j=1}^n [\sigma_{yy}^y(\xi_k, \eta_j) T_{i-1}(\eta_j)] b_i + \sigma^\infty = 0 \quad (2.32)$$

$$\sum_{i=1}^n \frac{\pi}{n} \sum_{j=1}^n [\sigma_{xy}^x(\xi_k, \eta_j) T_{i-1}(\eta_j)] a_i + \sum_{i=1}^n \frac{\pi}{n} \sum_{j=1}^n [\sigma_{xy}^y(\xi_k, \eta_j) T_{i-1}(\eta_j)] b_i = 0 \quad (2.33)$$

applying the no net dislocation condition

$$\int_{-a}^{+a} \psi_x(x') dx' = 0, \int_{-a}^{+a} \psi_y(x') dx' = 0 \quad (2.34)$$

or

$$\int_{-a}^{+a} \frac{g(x')}{\sqrt{(a^2 - x'^2)}} dx' = 0, \int_{-a}^{+a} \frac{f(x')}{\sqrt{(a^2 - x'^2)}} dx' = 0$$

in terms of non dimensional parameter

$$\int_{-1}^{+1} \frac{g(\eta)}{\sqrt{1-\eta^2}} d\eta = 0, \int_{-1}^{+1} \frac{f(\eta)}{\sqrt{1-\eta^2}} d\eta = 0 \quad (2.35)$$

$$\sum_{i=1}^n \left[\int_{-1}^{+1} \frac{T_{i-1}(\eta)}{\sqrt{1-\eta^2}} d\eta \right] a_i = 0, \sum_{i=1}^n \left[\int_{-1}^{+1} \frac{T_{i-1}(\eta)}{\sqrt{1-\eta^2}} d\eta \right] b_i = 0$$

$$\sum_{i=1}^n \frac{\pi}{n} \left[\sum_{j=1}^n T_{i-1}(\eta_j) \right] a_i = 0, \sum_{i=1}^n \frac{\pi}{n} \left[\sum_{j=1}^n T_{i-1}(\eta_j) \right] b_i = 0 \quad (2.36)$$

$$\begin{aligned} \text{where } \xi_k &= \cos k\pi/n, & k &= 1, n-1 \\ \eta_j &= \cos(\pi(2j-1)/2n), & j &= 1, n \end{aligned}$$

solving equation (2.31), (2.32) along with (2.37) for the unknowns

$$K_I = \frac{\mu}{2(1-\nu)} \lim_{\eta \rightarrow 1} \sqrt{2\pi(1-\eta)} [\psi_y(\eta)] \quad (2.37)$$

$$K_I = \frac{\mu}{2a(1-\nu)} \lim_{\eta \rightarrow 1} \sqrt{2\pi(1-\eta)} \left[\frac{\sum_{i=1}^n b_i T_{i-1}(\eta)}{\sqrt{1-\eta^2}} \right] \quad (2.38)$$

$$K_I = \frac{\mu}{2a(1-\nu)} \sqrt{\pi} \sum_{i=1}^n b_i \quad (2.39)$$

2.5.2 Analytical result:

$$K_I = P\sqrt{\pi a} \quad (2.40)$$

2.5.3 Comparison between Computational and Analytical Results

For $\mu = 80$ Gpa, $\nu = 0.3$, $P = 80$ MPa, $2a = 20$ mm

$$K_{I(\text{computational})} = 14.1796308 \text{ MPa} \sqrt{m}$$

$$K_{I(\text{analytical})} = 14.1796308 \text{ MPa} \sqrt{m}$$

while Chan et al. (1970) has obtained the results by FEM with an error of about 11% with coarse mesh, and about 5% with fine mesh.

2.6 The Mode-II crack :

2.6.1 Solution using Dislocations:

Mode-II crack is shown in the figure. The governing integral equation for this mode is same as that for mode I.

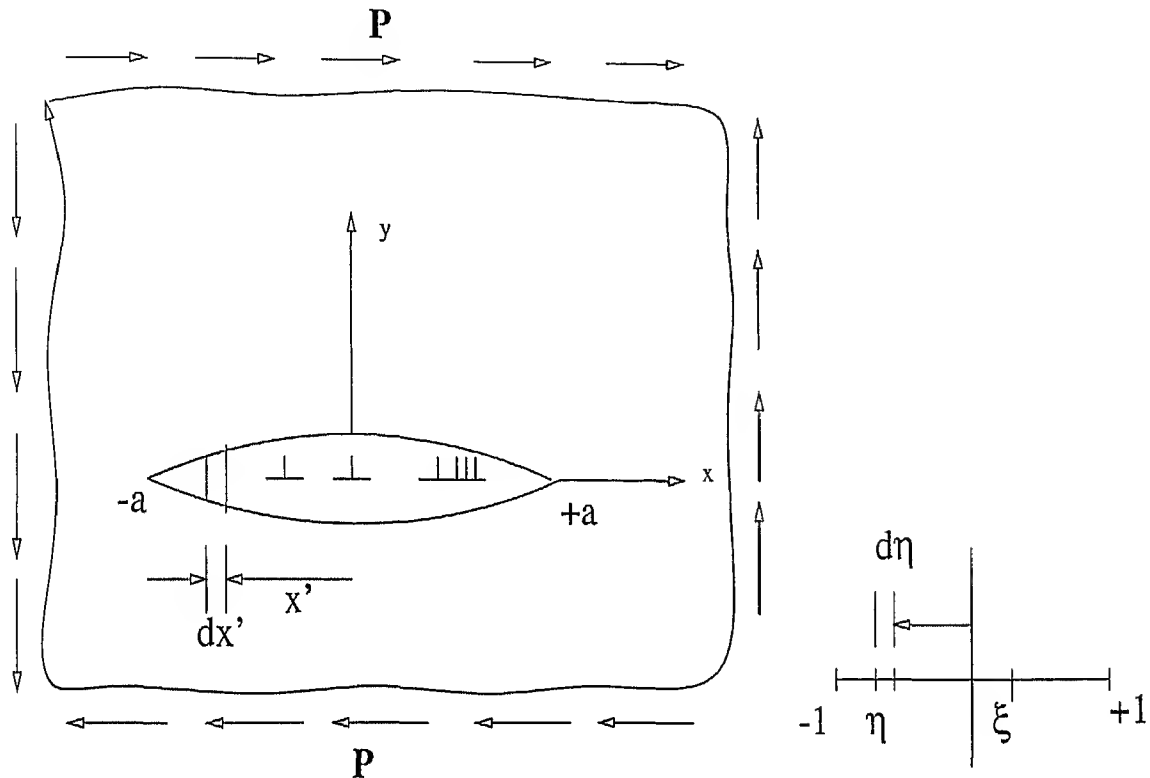


Figure 2.4: Mode-II crack subjected to far field P

$$\int_{-a}^{+a} \sigma_{yy}^x(x, x') \psi_x(x') dx' + \int_{-a}^{+a} \sigma_{yy}^y(x, x') \psi_y(x') dx' = 0 \quad (2.41)$$

$$\int_{-a}^{+a} \sigma_{xy}^x(x, x') \psi_x(x') dx' + \int_{-a}^{+a} \sigma_{xy}^y(x, x') \psi_y(x') dx' + \tau^\infty = 0 \quad (2.42)$$

$$\psi_x(x') = \frac{g(x')}{\sqrt{(a^2 - x^2)}}, \psi_y(x') = \frac{f(x')}{\sqrt{(a^2 - x^2)}} \quad (2.43)$$

rewriting the equation,

$$\int_{-a}^{+a} \sigma_{yy}^x(x, x') \frac{g(x')}{\sqrt{(a^2 - x^2)}} dx' + \int_{-a}^{+a} \sigma_{yy}^y(x, x') \frac{f(x')}{\sqrt{(a^2 - x^2)}} dx' = 0 \quad (2.44)$$

$$\int_{-a}^{+a} \sigma_{xy}^x(x, x') \frac{g(x')}{\sqrt{(a^2 - x^2)}} dx' + \int_{-a}^{+a} \sigma_{xy}^y(x, x') \frac{f(x')}{\sqrt{(a^2 - x^2)}} dx' + \tau^\infty = 0 \quad (2.45)$$

writing the above equation in non dimensional terms

$$\int_{-1}^{+1} \frac{\sigma_{yy}^x(\xi, \eta)}{\sqrt{(1 - \eta^2)}} g(\eta) d\eta + \int_{-1}^{+1} \frac{\sigma_{yy}^y(\xi, \eta)}{\sqrt{(1 - \eta^2)}} f(\eta) d\eta = 0 \quad (2.46)$$

$$\int_{-1}^{+1} \frac{\sigma_{xy}^x(\xi, \eta)}{\sqrt{(1 - \eta^2)}} g(\eta) d\eta + \int_{-1}^{+1} \frac{\sigma_{xy}^y(\xi, \eta)}{\sqrt{(1 - \eta^2)}} f(\eta) d\eta + \tau^\infty = 0 \quad (2.47)$$

representing $g(\eta)$, $f(\eta)$ in terms of unknown coefficient and known functions

$$g(\eta) = \sum_{i=1}^n a_i T_{i-1}(\eta), f(\eta) = \sum_{i=1}^n b_i T_{i-1} \quad (2.48)$$

writing the above equation in non dimensional terms

$$\int_{-1}^{+1} \sigma_{yy}^x(\xi, \eta) \psi(\eta) d\eta + \int_{-1}^{+1} \sigma_{yy}^y(\xi, \eta) \psi(\eta) d\eta = 0 \quad (2.49)$$

$$\int_{-1}^{+1} \sigma_{xy}^x(\xi, \eta) \psi(\eta) d\eta + \int_{-1}^{+1} \sigma_{xy}^y(\xi, \eta) \psi(\eta) d\eta + \tau^\infty = 0 \quad (2.50)$$

applying the quadrature rule

$$\sum_{i=1}^n \frac{\pi}{n} \sum_{j=1}^n [\sigma_{yy}^x(\xi_k, \eta_j) T_{i-1}(\eta_j)] a_i + \sum_{i=1}^n \frac{\pi}{n} \sum_{j=1}^n [\sigma_{yy}^y(\xi_k, \eta_j) T_{i-1}(\eta_j)] b_i = 0 \quad (2.51)$$

$$\sum_{i=1}^n \frac{\pi}{n} \sum_{j=1}^n [\sigma_{xy}^x(\xi_k, \eta_j) T_{i-1}(\eta_j)] a_i + \sum_{i=1}^n \frac{\pi}{n} \sum_{j=1}^n [\sigma_{xy}^y(\xi_k, \eta_j) T_{i-1}(\eta_j)] b_i + \tau^\infty = 0 \quad (2.52)$$

applying the no net dislocation condition

$$\int_{-a}^{+a} \psi_x(x') dx' = 0, \int_{-a}^{+a} \psi_y(x') dx' = 0 \quad (2.53)$$

or

$$\int_{-a}^{+a} \frac{g(x')}{\sqrt{(a^2 - x'^2)}} dx' = 0, \int_{-a}^{+a} \frac{f(x')}{\sqrt{(a^2 - x'^2)}} dx' = 0 \quad (2.54)$$

in terms of non dimensional parameter

$$\int_{-1}^{+1} \frac{g(\eta)}{\sqrt{1 - \eta^2}} d\eta = 0, \int_{-1}^{+1} \frac{f(\eta)}{\sqrt{1 - \eta^2}} d\eta = 0 \quad (2.55)$$

$$\sum_{i=1}^n \left[\int_{-1}^{+1} \frac{T_{i-1}(\eta)}{\sqrt{1 - \eta^2}} d\eta \right] a_i = 0, \sum_{i=1}^n \left[\int_{-1}^{+1} \frac{T_{i-1}(\eta)}{\sqrt{1 - \eta^2}} d\eta \right] b_i = 0 \quad (2.56)$$

$$\sum_{i=1}^n \frac{\pi}{n} \left[\sum_{j=1}^n T_{i-1}(\eta_j) \right] a_i = 0, \sum_{i=1}^n \frac{\pi}{n} \left[\sum_{j=1}^n T_{i-1}(\eta_j) \right] b_i = 0 \quad (2.57)$$

where $\xi_k = \cos k\pi/n$, $k=1, n-1$

$\eta_j = \cos(\pi(2j-1)/2n)$, $j=1, n$

solving (2.52), (2.53) along with (2.58) for the unknowns, and computing the stress intensity factor with the help of formula (2.61) given below,

$$K_{II} = \frac{\mu}{2(1-\nu)} \lim_{\eta \rightarrow 1} \sqrt{2\pi(1-\eta)} [\psi_x(\eta)] \quad (2.58)$$

$$K_{II} = \frac{\mu}{2a(1-\nu)} \lim_{\eta \rightarrow 1} \sqrt{2\pi(1-\eta)} \left[\frac{\sum_{i=1}^n a_i T_{i-1}(\eta)}{\sqrt{1-\eta^2}} \right] \quad (2.59)$$

$$K_{II} = \frac{\mu}{2a(1-\nu)} \sqrt{\pi} \sum_{i=1}^n a_i \quad (2.60)$$

2.6.2 Analytical Result:

$$K_{II} = P\sqrt{\pi a} \quad (2.61)$$

2.6.3 Comparison between Analytical and Computational Results

For $\mu = 80$ GPa, $\nu = 0.3$, $P = 80$ MPa, $2a = 20$ mm

$$K_{II(\text{computational})} = 14.1796308 \text{ MPa} \sqrt{m}$$

$$K_{II(\text{analytical})} = 14.1796308 \text{ MPa} \sqrt{m}$$

2.7 Arc shaped crack :

2.7.1 Solution using Dislocation:

The governing integral equation for a arc shaped crack is written below. where we are computing the stress field at a point θ because of a dislocation located at an angle ϕ , and the crack is subjected to uniform pressure.

$$\int_{-\alpha}^{+\alpha} \sigma_{rr}^{\rho}(\theta, \phi) \psi_{\rho}(\phi) d\phi + \int_{-\alpha}^{+\alpha} \sigma_{rr}^t(\theta, \phi) \psi_t(\phi) d\phi + \sigma_{rr}(\phi) = 0 \quad (2.62)$$

$$\int_{-\alpha}^{+\alpha} \sigma_{r\theta}^{\rho}(\theta, \phi) \psi_{\rho}(\phi) d\phi + \int_{-\alpha}^{+\alpha} \sigma_{r\theta}^t(\theta, \phi) \psi_t(\phi) d\phi + \sigma_{r\theta}(\phi) = 0 \quad (2.63)$$

where superscript 'ρ' and 't' are used for the dislocations with Burgers vector in *radial* and *tangential* direction respectively.

2α : Included arc angle.

$$\psi_{\rho}(\phi) = \frac{g(\phi)}{\sqrt{(\alpha^2 - \phi^2)}}, \psi_t(\phi) = \frac{f(\phi)}{\sqrt{(\alpha^2 - \phi^2)}} \quad (2.64)$$

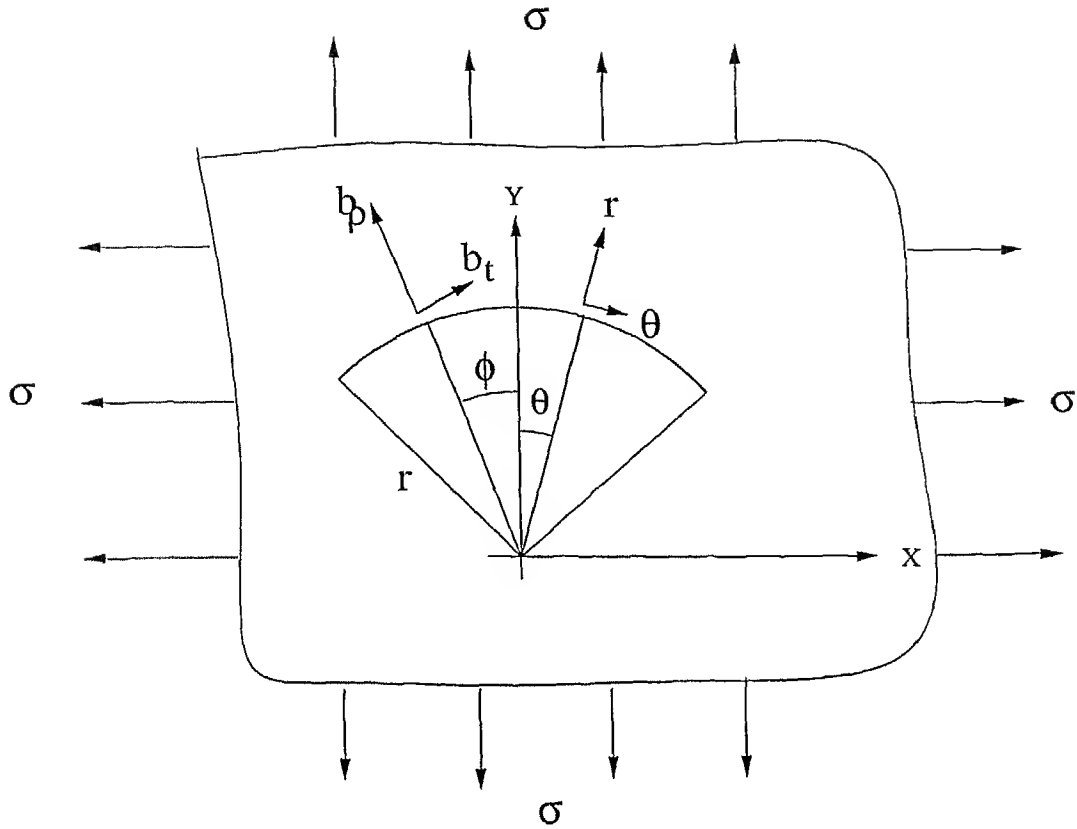


Figure 2.5: Arc shaped crack subjected to uniform pressure

rewriting the equations

$$\int_{-\alpha}^{-1} \sigma_{rr}^p(\theta, \phi) \frac{g(\phi)}{\sqrt{\alpha^2 - \phi^2}} d\phi + \int_{-\alpha}^{+\alpha} \sigma_{rr}^t(\theta, \phi) \frac{f(\phi)}{\sqrt{\alpha^2 - \phi^2}} d\phi + \sigma_{rr}(\phi) = 0 \quad (2.65)$$

$$\int_{-\alpha}^{-1} \sigma_{r\theta}^p(\theta, \phi) \frac{g(\phi)}{\sqrt{\alpha^2 - \phi^2}} d\phi + \int_{-\alpha}^{+\alpha} \sigma_{r\theta}^t(\theta, \phi) \frac{f(\phi)}{\sqrt{\alpha^2 - \phi^2}} d\phi + \sigma_{r\theta}(\phi) = 0 \quad (2.66)$$

in terms of non dimensional parameters

$$\int_{-1}^{+1} \sigma_{rr}^p(\xi, \eta) \frac{g(\eta)}{\sqrt{1 - \eta^2}} d\eta + \int_{-1}^{+1} \sigma_{rr}^t(\xi, \eta) \frac{f(\eta)}{\sqrt{1 - \eta^2}} d\eta + \sigma_{rr}(\xi) = 0 \quad (2.67)$$

$$\int_{-1}^{+1} \sigma_{r\theta}^p(\xi, \eta) \frac{g(\eta)}{\sqrt{1 - \eta^2}} d\eta + \int_{-1}^{+1} \sigma_{r\theta}^t(\xi, \eta) \frac{f(\eta)}{\sqrt{1 - \eta^2}} d\eta + \sigma_{r\theta}(\xi) = 0 \quad (2.68)$$

$g(\eta)$, $f(\eta)$ can be expanded in terms of chebyshev polynomials with unknown coefficients a_i and b_i .

$$g(\eta) = \sum_{i=1}^n a_i T_{i-1}(\eta), f(\eta) = \sum_{i=1}^n b_i T_{i-1} \quad (2.69)$$

$$\sum_{i=1}^n \left[\int_{-1}^{+1} \frac{\sigma_{rr}^p(\xi, \eta)}{\sqrt{1 - \eta^2}} T_{i-1}(\eta) d\eta \right] a_i + \sum_{i=1}^n \left[\int_{-1}^{+1} \frac{\sigma_{rr}^t(\xi, \eta)}{\sqrt{1 - \eta^2}} T_{i-1}(\eta) d\eta \right] b_i + \sigma_{rr} = 0 \quad (2.70)$$

$$\sum_{i=1}^n \left[\int_{-1}^{+1} \frac{\sigma_{r\theta}^{\rho}(\xi, \eta)}{\sqrt{1-\eta^2}} T_{i-1}(\eta) d\eta \right] a_i + \sum_{i=1}^n \left[\int_{-1}^{+1} \frac{\sigma_{r\theta}^t(\xi, \eta)}{\sqrt{1-\eta^2}} T_{i-1}(\eta) d\eta \right] b_i + \sigma_{r\theta} = 0 \quad (2.71)$$

applying the quadrature rule,

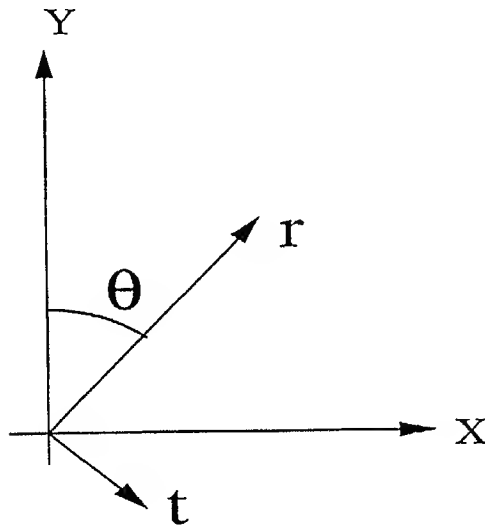
$$\sum_{i=1}^n \frac{\pi}{n} \sum_{j=1}^n [\sigma_{rr}^{\rho}(\xi_k, \eta_j) T_{i-1}(\eta_j)] a_i + \sum_{i=1}^n \frac{\pi}{n} \sum_{j=1}^n [\sigma_{rr}^t(\xi_k, \eta_j) T_{i-1}(\eta_j)] b_i + \sigma_{rr}(\xi_k) = 0 \quad (2.72)$$

$$\sum_{i=1}^n \frac{\pi}{n} \sum_{j=1}^n [\sigma_{r\theta}^{\rho}(\xi_k, \eta_j) T_{i-1}(\eta_j)] a_i + \sum_{i=1}^n \frac{\pi}{n} \sum_{j=1}^n [\sigma_{r\theta}^t(\xi_k, \eta_j) T_{i-1}(\eta_j)] b_i + \sigma_{r\theta}(\xi_k) = 0 \quad (2.73)$$

no net dislocation condition in global (x,y) set

$$\int_{-\alpha}^{+\alpha} \psi_x(\phi) d\phi = 0 \quad (2.74)$$

applying the transformation,



$$\begin{bmatrix} x \\ y \end{bmatrix} = \begin{bmatrix} \sin \theta & \cos \theta \\ \cos \theta & -\sin \theta \end{bmatrix} \begin{bmatrix} r \\ t \end{bmatrix}$$

Figure 2.6: Rotation Matrix

$$\int_{-\alpha}^{+\alpha} [\psi_r(\phi) \sin(\phi) + \psi_t(\phi) \cos(\phi)] d\phi = 0 \quad (2.75)$$

or

$$\int_{-\alpha}^{+\alpha} \frac{g(\phi)}{\sqrt{(\alpha^2 - \phi^2)}} \sin(\phi) + \frac{f(\phi)}{\sqrt{(\alpha^2 - \phi^2)}} \cos(\phi) d\phi = 0 \quad (2.76)$$

in terms of non dimensional parameter

$$\int_{-1}^{+1} \left[\frac{g(\eta)}{\sqrt{1-\eta^2}} \sin(\eta\alpha) + \frac{f(\eta)}{\sqrt{1-\eta^2}} \cos(\eta\alpha) \right] d\eta = 0 \quad (2.77)$$

$$\sum_{i=1}^n \left[\int_{-1}^{+1} \frac{T_{i-1}(\eta)}{\sqrt{1-\eta^2}} \sin(\eta\alpha) d\eta \right] a_i + \sum_{i=1}^n \left[\int_{-1}^{+1} \frac{T_{i-1}(\eta)}{\sqrt{1-\eta^2}} \cos(\eta\alpha) d\eta \right] b_i = 0 \quad (2.78)$$

$$\sum_{i=1}^n \frac{\pi}{\eta_i} \left[\sum_{j=1}^n T_{i-1}(\eta_j) \sin(\eta_j \alpha) \right] a_i + \sum_{i=1}^n \frac{\pi}{\eta_i} \left[\sum_{j=1}^n T_{i-1}(\eta_j) \cos(\eta_j \alpha) \right] b_i = 0 \quad (2.79)$$

for the no net dislocation in y-direction

$$\int_{-\alpha}^{+\alpha} \psi_y(\phi) d\phi = 0 \quad (2.80)$$

$$\int_{-\alpha}^{+\alpha} [\psi_\rho(\phi) \cos(\phi) - \psi_t(\phi) \sin(\phi)] d\phi = 0 \quad (2.81)$$

following the similar steps

$$\sum_{i=1}^n \frac{\pi}{\eta_i} \left[\sum_{j=1}^n T_{i-1}(\eta_j) \cos(\eta_j \alpha) \right] a_i - \sum_{i=1}^n \frac{\pi}{\eta_i} \left[\sum_{j=1}^n T_{i-1}(\eta_j) \sin(\eta_j \alpha) \right] b_i = 0 \quad (2.82)$$

where $\xi_k = \cos k\pi/n$, $k=1, n-1$

$\eta_j = \cos(\pi(2j-1)/2n)$, $j=1, n$

in terms of non dimensional parameter SIF is given as

$$K_{II} + iK_I = \frac{\mu}{2(1-\nu)} \lim_{\eta \rightarrow 1} \sqrt{2\pi(1-\eta)} [\psi_t(\eta) + i\psi_\rho(\eta)] \quad (2.83)$$

$$K_{II} + iK_I = \frac{\mu}{2a(1-\nu)} \sqrt{\pi} [\sum_{i=1}^n a_i + i\sum_{i=1}^n b_i] \quad (2.84)$$

2.7.2 Analytical Result:

$$K_{IA} = \sigma \sqrt{\pi r \sin \alpha} \frac{\cos \frac{\alpha}{2}}{1 + \sin^2 \frac{\alpha}{2}} \quad (2.85)$$

$$K_{IIA} = \sigma \sqrt{\pi r \sin \alpha} \frac{\sin \frac{\alpha}{2}}{1 + \sin^2 \frac{\alpha}{2}} \quad (2.86)$$

2.7.3 Comparison between Computational and Analytical results

For $\mu = 80$ GPa, $\nu = 0.3$, $\sigma = 1$ MPa, $r = 0.05$ m, $2\alpha = 180$ degrees

$K_{I(computational)} = 0.186833041$ MPa \sqrt{m}

$K_{I(analytical)} = 0.186833041$ MPa \sqrt{m}

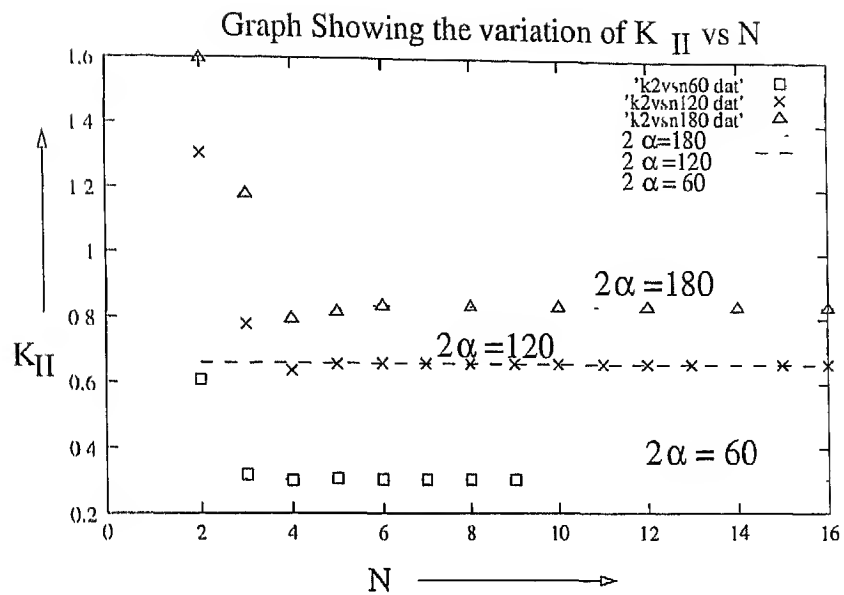


Figure 2.7: Graph Showing the variation of K_{II} vs N :

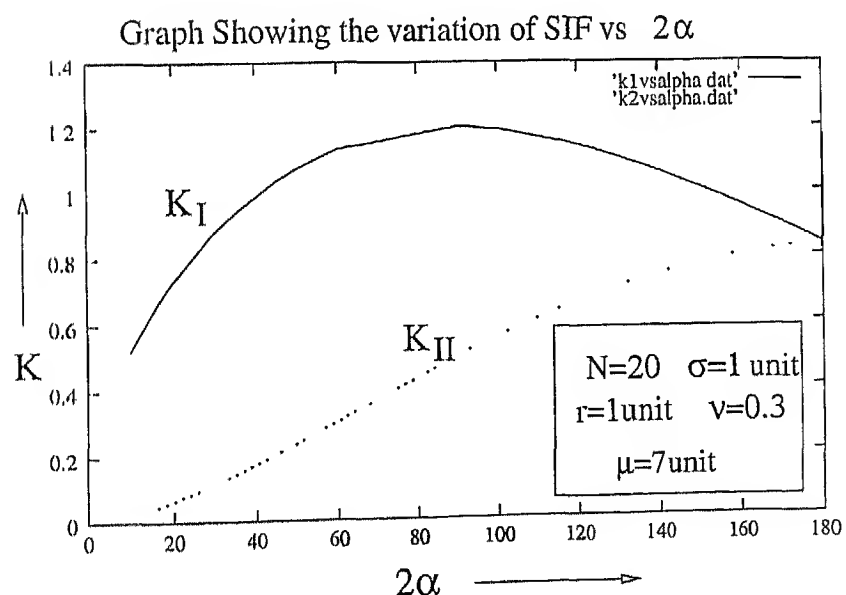


Figure 2.8: Graph Showing the variation of SIF vs 2α :

Chapter 3

Complex geometries

3.1 Bi-Periodic cracks:

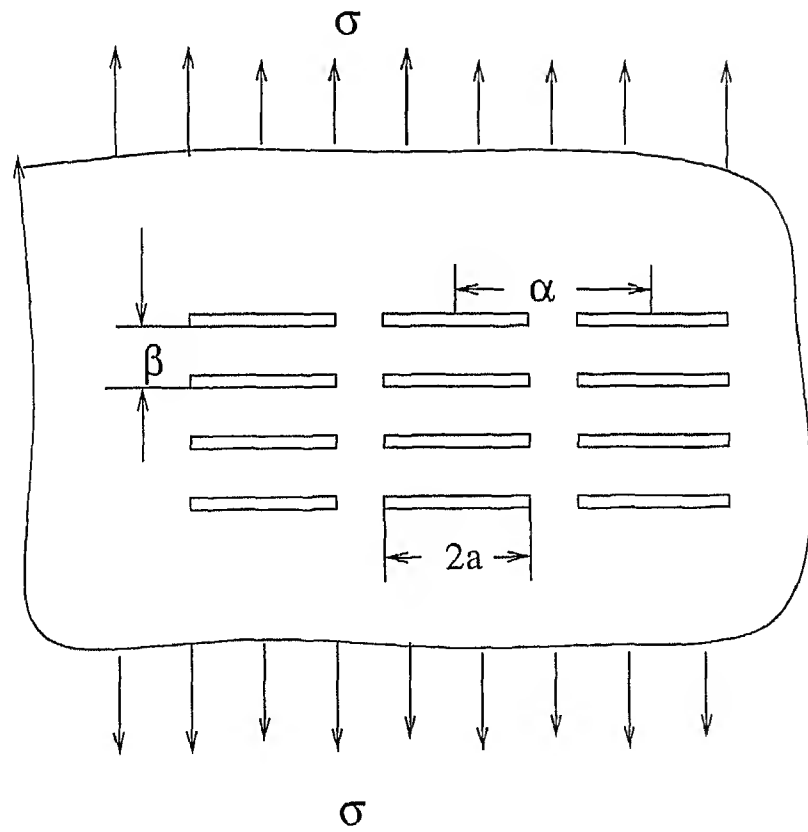


Figure 3.1: Bi periodic cracks in an infinite body with periodicity α in x-direction and β in Y-direction:

Fig(3.1) shows bi-periodic cracks in an infinite body with periodicity α and β in X and Y direction respectively subjected to far field stress σ an τ . The stress field of dislocation for this case is taken from reference-[7]. Graph shows the variation of stress intensity factor with

parameter α and β respectively.

3.1.1 Array of cracks with periodicity Alpha in X-direction:

Fig(3.2) shows the periodic array of cracks with periodicity α in x-direction(when β is much greater than α). variation of SIF with respect to different values of α and β is given in the graphs

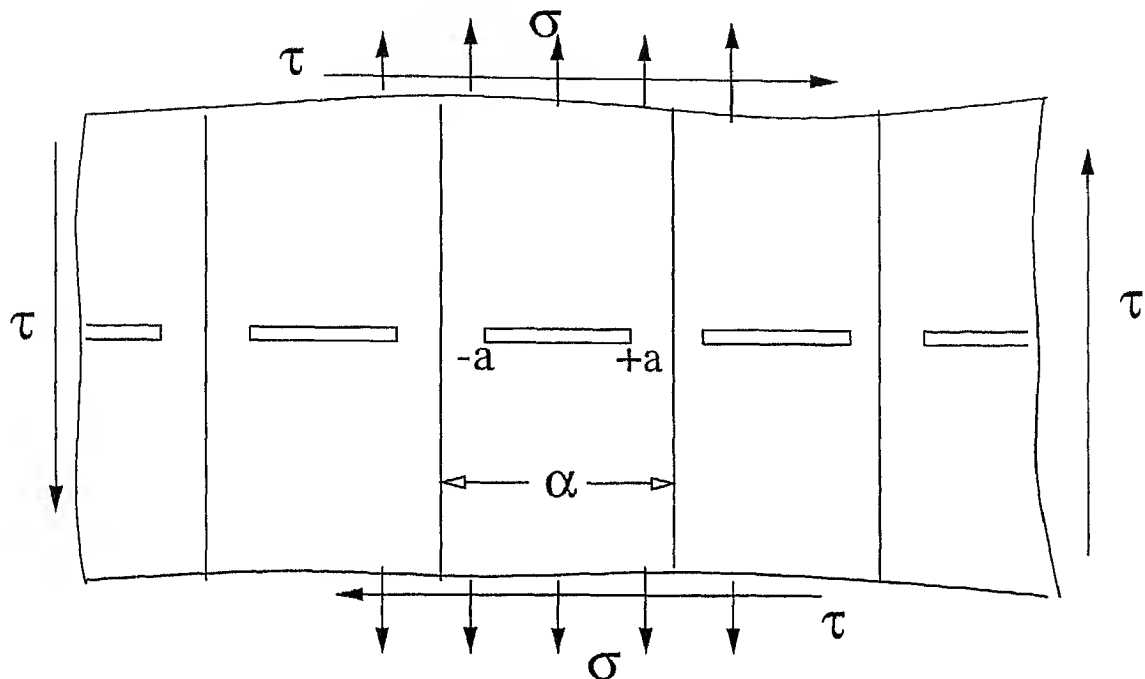


Figure 3.2: Array of cracks in an infinite body with periodicity α in x-direction where $\beta \gg \alpha$

3.1.2 Array of cracks with periodicity Beta in Y-direction:

Fig(3.4) shows the periodic array of cracks with periodicity α in x-direction(when α is much greater than β). variation of SIF with respect to different values of α and β is given in the graphs.

actual data for KI are taken by Fourier Transform (Fichter),Expansion of Complex Potential(Isida),Asymptotic Approximation (Polynomial of degree ten)(Benthem). Accuracy of these data is about 2%.

3.2 Circular inclusion with interface

In composite materials containing fiber or particulate reinforcement the interface separating matrix from inclusion is widely believed to be a dominant influence affecting the overall stiffness and

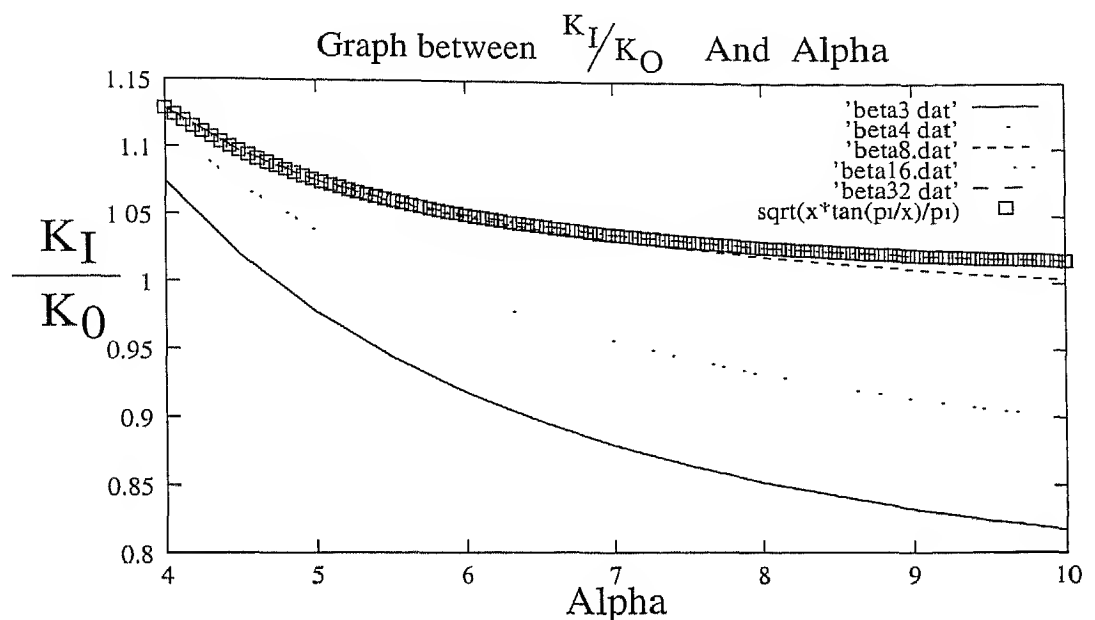


Figure 3.3: Graphs showing the variation of K_I/K_0 vs periodicity in x direction i.e. Alpha for different values of beta

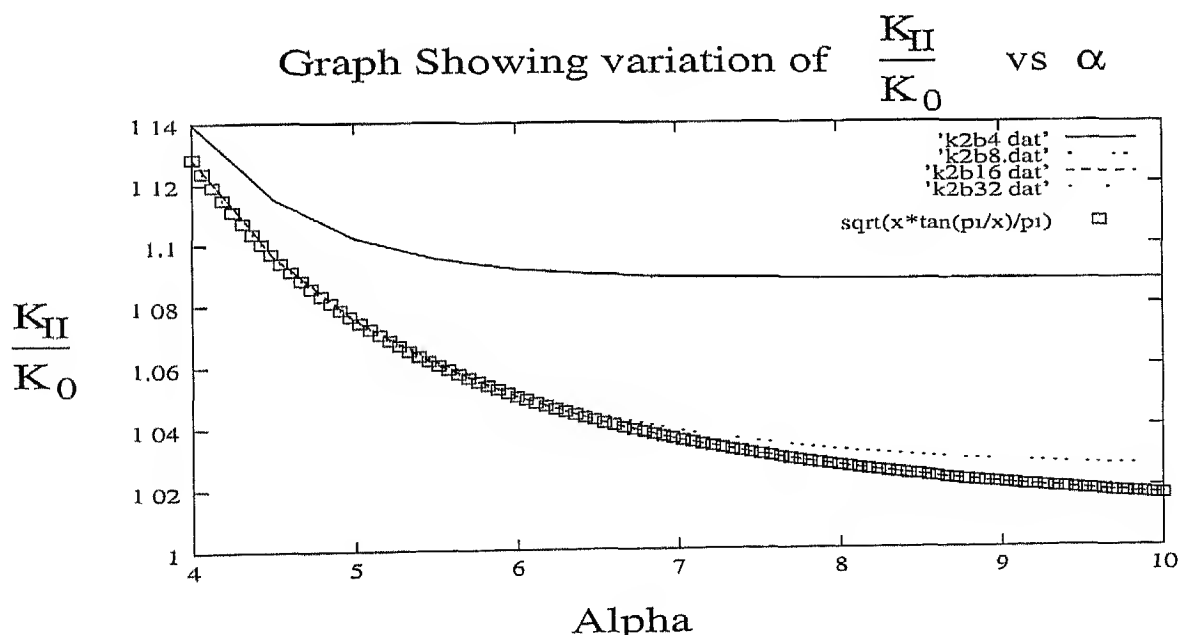


Figure 3.4: Graphs showing the variation of K_{II}/K_0 vs periodicity in x direction i.e. Alpha for different values of beta

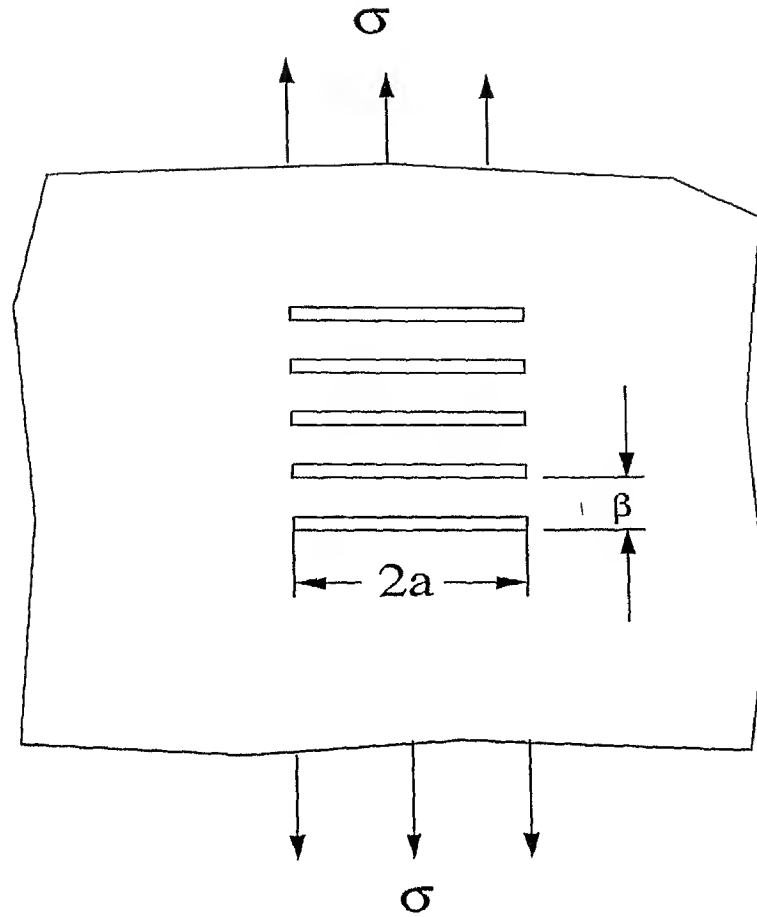


Figure 3.5: Array of cracks in an infinite body with periodicity beta in y-direction

damage tolerance characteristics of the composite. Damage accumulation in a composite often depends on the character of the mechanical response of the interface. Hence accurate assessment of the overall stiffness characteristics of a composite containing fiber bonded to the matrix is an extremely important in the attempt to obtain improved composite performance.

Standard material models require for their implementation the solution to a solitary inclusion-interface-matrix system the problem of obtaining effective material properties for a composite is, to a large extent, dependent on the availability of the elastic field solutions to the solitary problem.

3.2.1 Interface Law

The interface separating the matrix from inclusion is characterized by a constitutive equation relating the components of interface traction to components of interface displacement jump. If only normal inter-sfacial traction develops from the normal component of displacement jump then,

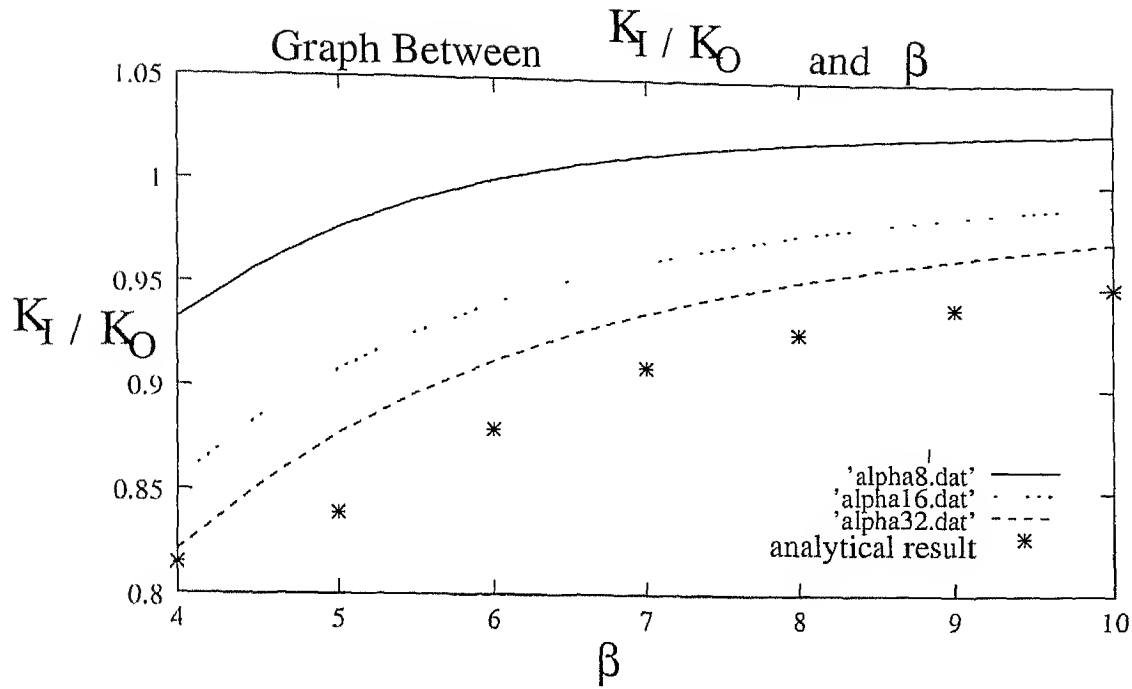


Figure 3.6: Graphs showing the variation of K_I/K_O vs periodicity in y direction i.e. Beta for different values of Alpha

owing to rotational symmetry, the force law assumes the form

$$S(\mathbf{n}) = f([u_r])\mathbf{n}$$

where $S(\mathbf{n})$ is the interface traction vector acting on the interface and f is a scalar function of radial interface displacement jump $[u_r]$.

3.2.2 Problem Formulation

consider a circular inclusion-interface-matrix system subjected to uniform pressure σ , where 'r' is the radius of the circular inclusion.

The governing integral equations for a circular inclusion problem is given below.

$$\int_0^{2\pi} \sigma_{rr}^p(\theta, \phi) \psi_p(\phi) d\phi + \int_0^{2\pi} \sigma_{rr}^t(\theta, \phi) \psi_t(\phi) d\phi + \sigma_{rr}^a(\theta) + \sigma_{rr}^c(u_r(\theta), u_t(\theta)) = 0 \quad (3.1)$$

$$\int_0^{2\pi} \sigma_{r\theta}^p(\theta, \phi) \psi_p(\phi) d\phi + \int_0^{2\pi} \sigma_{r\theta}^t(\theta, \phi) \psi_t(\phi) d\phi + \sigma_{r\theta}^a(\theta) + \sigma_{r\theta}^c(u_r(\theta), u_t(\theta)) = 0 \quad (3.2)$$

where superscript 'a' indicates the stress field because of applied pressure, and 'c' indicates the stress field because of inter-facial bonding, i.e. cohesive zones.

$u_r(\theta)$ is used for *jump-in-displacement* in radial direction at the point θ .

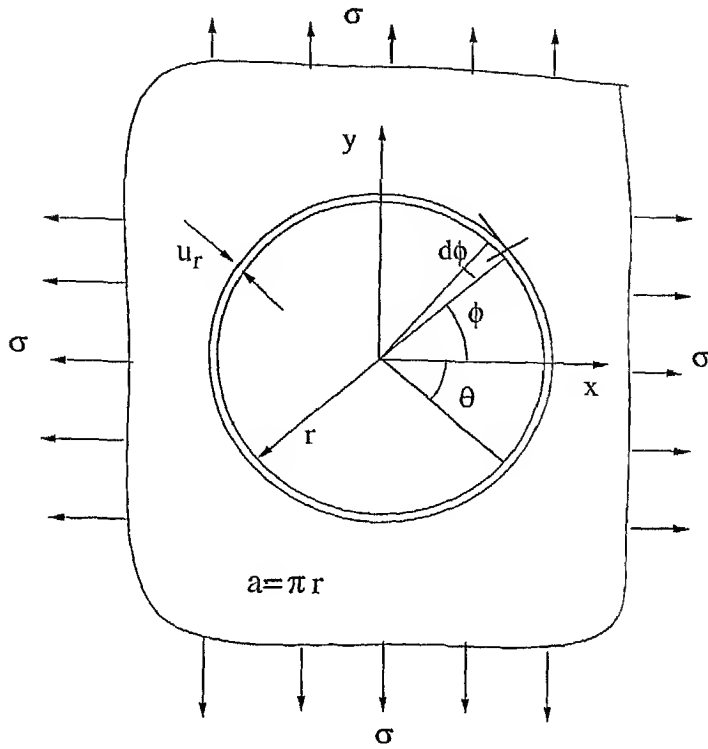


Figure 3.7: A circular inclusion subjected to uniform far field pressure σ

similarly $u_t(\theta)$ indicates *jump-in-displacement* along tangential direction at the point θ , writing the above equations in non-dimensional terms and making use of *interface law*,

$$a \int_{-1}^{+1} \sigma_{rr}^p(\xi, \eta) \psi_p(\eta) d\eta + a \int_{-1}^{+1} \sigma_{rr}^t(\xi, \eta) \psi_t(\eta) d\eta + \sigma_{rr}^a(\xi) + Ku_r(\xi) = 0 \quad (3.3)$$

$$a \int_{-1}^{+1} \sigma_{r\theta}^p(\xi, \eta) \psi_p(\eta) d\eta + a \int_{-1}^{+1} \sigma_{r\theta}^t(\xi, \eta) \psi_t(\eta) d\eta + \sigma_{r\theta}^a(\xi) + Ku_t(\xi) = 0 \quad (3.4)$$

where, $\sigma_{rr}^c(u_r(\xi), u_t(\xi)) = Ku_r(\xi)$, $\sigma_{r\theta}^c(u_r(\xi), u_t(\xi)) = Ku_t(\xi)$

K : Interface Modulus

$$u_x(\xi) = a_0 + a \int_{-1}^{\xi} \psi_x(\eta) d\eta$$

where, a_O : *Jump - in - displacement* at $(r, 0)$

$$u_x(\xi) = a_0 + a \int_{-1}^{\xi} [\psi_p(\eta) \cos \theta - \psi_t(\eta) \sin \theta] d\eta$$

expressing dislocation densities in terms of unknown coefficients and chebyshev polynomials

$$\psi_p(\eta) = \sum_{p=0}^{n-2} a_p T_p(\eta) \psi_t(\eta) = \sum_{p=0}^{n-2} b_p T_p(\eta)$$

$$u_x(\xi) = a_0 + a \sum_{p=0}^{n-2} a_p \left[\int_{-1}^{\xi} T_p(\eta) \cos \theta d\eta \right] - a \sum_{p=0}^{n-2} b_p \left[\int_{-1}^{\xi} T_p(\eta) \sin \theta d\eta \right]$$

applying the quadrature rule,

$$\begin{aligned} u_x(\xi) &= a_0 + a \sum_{p=0}^{n-2} a_p \sum_{j=1}^n H(\xi, \eta_j) T_p(\eta_j) \cos \theta_j \sqrt{1 - \eta_j^2} \\ &\quad - a \sum_{p=0}^{n-2} a_p \sum_{j=1}^n H(\xi, \eta_j) T_p(\eta_j) \sin \theta_j \sqrt{1 - \eta_j^2} \end{aligned} \quad (3.5)$$

where

$$H(\xi, \eta) = \begin{cases} 0, & \text{for } \xi < \eta \\ 1, & \text{for } -1 \leq \eta \leq \xi \end{cases}$$

similarly

$$u_y(\xi) = b_0 + a \int_{-1}^{\xi} \psi_y(\eta) d\eta$$

where, b_0 : Jump - in - displacement at $(r, 0)$

$$u_y(\xi) = b_0 + a \int_{-1}^{\xi} [\psi_p(\eta) \sin \theta + \psi_t(\eta) \cos \theta] d\eta$$

expressing dislocation densities in terms of chebyshev polynomial and applying the quadrature rule,

$$\begin{aligned} u_y(\xi) &= b_0 + a \sum_{p=0}^{n-2} a_p \sum_{j=1}^n H(\xi, \eta_j) T_p(\eta_j) \sin \theta_j \sqrt{1 - \eta_j^2} \\ &\quad + a \sum_{p=0}^{n-2} a_p \sum_{j=1}^n H(\xi, \eta_j) T_p(\eta_j) \cos \theta_j \sqrt{1 - \eta_j^2} \end{aligned} \quad (3.6)$$

$$u_r(\xi) = u_x(\xi) \cos \theta_\xi + u_y(\xi) \sin \theta_\xi \quad (3.7)$$

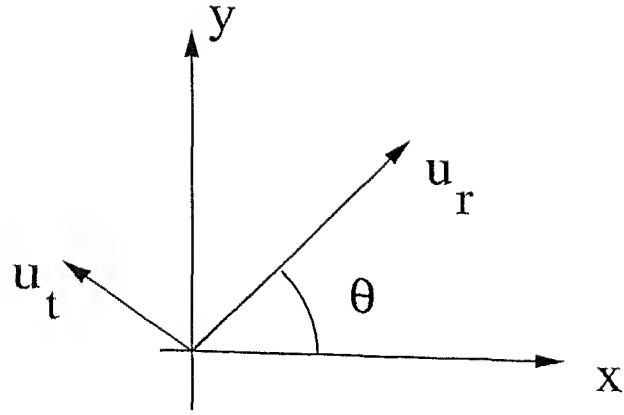
applying the transformation

$$\begin{aligned} u_r(\xi) &= a_0 \cos \theta + b_0 \sin \theta + a \sum_{p=0}^{n-2} a_p \frac{\pi}{n} \sum_{j=1}^n H(\xi, \eta_j) T_p(\eta_j) \sqrt{1 - \eta_j^2} \cos(\theta_\xi - \theta_j) \\ &\quad + a \sum_{p=0}^{n-2} b_p \frac{\pi}{n} \sum_{j=1}^n H(\xi, \eta_j) T_p(\eta_j) \sqrt{1 - \eta_j^2} \sin(\theta_\xi - \theta_j) \end{aligned} \quad (3.8)$$

$$u_t(\xi) = -\sin \theta_\xi u_x(\xi) + \cos \theta_\xi u_y(\xi) \quad (3.9)$$

substituting the values of u_x and u_y in the expression of u_t

$$\begin{aligned} u_t(\xi) &= -a_0 \sin \theta_\xi + b_0 \cos \theta_\xi - a \sum_{p=0}^{n-2} a_p \frac{\pi}{n} \sum_{j=1}^n H(\xi, \eta_j) T_p(\eta_j) \sqrt{1 - \eta_j^2} \sin(\theta_\xi - \theta_j) \\ &\quad + a \sum_{p=0}^{n-2} b_p \frac{\pi}{n} \sum_{j=1}^n H(\xi, \eta_j) T_p(\eta_j) \sqrt{1 - \eta_j^2} \cos(\theta_\xi - \theta_j) \end{aligned} \quad (3.10)$$



$$\begin{bmatrix} u_r \\ u_t \end{bmatrix} = \begin{bmatrix} \cos \theta & \sin \theta \\ -\sin \theta & \cos \theta \end{bmatrix} \begin{bmatrix} u_x \\ u_y \end{bmatrix}$$

Figure 3.8: Rotation Matrix

substituting the values of u_r and u_t in the governing integral equations and making use of quadrature rule, after readjusting the terms the equations become

$$\begin{aligned} & \sum_{p=0}^n a_p \frac{\pi}{\eta_l} \sum_{j=1}^n T_p(\eta_j) \sqrt{1 - \eta_j^2} a [\sigma_{rr}^p(\xi_k, \eta_j) + KH(\xi_k, \eta_j) \cos(\theta_\xi - \theta_j)] \\ & + \sum_{p=0}^n b_p \frac{\pi}{\eta_l} \sum_{j=1}^n T_p(\eta_j) \sqrt{1 - \eta_j^2} a [\sigma_{rr}^t(\xi_k, \eta_j) + KH(\xi_k, \eta_j) \sin(\theta_\xi - \theta_j)] \\ & + K \cos \theta_\xi a_0 + K \sin \theta_\xi b_0 = -\sigma_{rr}^a(\xi_k) \end{aligned} \quad (3.11)$$

$$\begin{aligned} & \sum_{p=0}^n a_p \frac{\pi}{\eta_l} \sum_{j=1}^n T_p(\eta_j) \sqrt{1 - \eta_j^2} a [\sigma_{r\theta}^p(\xi_k, \eta_j) - KH(\xi_k, \eta_j) \sin(\theta_\xi - \theta_j)] \\ & + \sum_{p=0}^n b_p \frac{\pi}{\eta_l} \sum_{j=1}^n T_p(\eta_j) \sqrt{1 - \eta_j^2} a [\sigma_{rr}^t(\xi_k, \eta_j) + KH(\xi_k, \eta_j) \cos(\theta_\xi - \theta_j)] \\ & - K \sin \theta_\xi a_0 + K \cos \theta_\xi b_0 = -\sigma_{r\theta}^a(\xi_k) \end{aligned} \quad (3.12)$$

imposing the no net dislocation condition in global (x,y) coordinate system

$$\begin{aligned} & \int_{-1}^{+1} \psi_x(\eta) d\eta = 0 \\ & \int_{-1}^{+1} [\cos \theta_j \psi_\rho(\eta) - \sin \theta_j \psi_t(\eta)] d\eta \end{aligned}$$

applying the quadrature rule,

$$\sum_{p=0}^{n-2} a_p \frac{\pi}{n} \sum_{j=1}^n T_p(\eta_j) \cos \theta_j \sqrt{1 - \eta^2} - \sum_{p=0}^{n-2} b_p \frac{\pi}{n} \sum_{j=1}^n T_p(\eta_j) \sin \theta_j \sqrt{1 - \eta^2} = 0 \quad (3.13)$$

similarly for y dislocation,

$$\int_{-1}^{+1} \psi(\eta) d\eta = \int_{-1}^{+1} [\sin \theta_j \psi_p(\eta) + \cos \theta_j \psi_t(\eta)] d\eta = 0$$

applying the quadrature rule,

$$\sum_{p=0}^{n-2} a_p \frac{\pi}{n} \sum_{j=1}^n T_p(\eta_j) \sin \theta_j \sqrt{1 - \eta^2} + \sum_{p=0}^{n-2} b_p \frac{\pi}{n} \sum_{j=1}^n T_p(\eta_j) \cos \theta_j \sqrt{1 - \eta^2} = 0 \quad (3.14)$$

equation (3.11), (3.12), (3.13) and (3.14) now solved for unknowns. once the unknowns are determined one can compute the jump-in-displacement at any point on the circular inclusion by using the equation (3.7) and (3.9) respectively.

3.2.3 Analytical Result

For the plain strain problems the displacement vector in radial direction U_r is given by:

$$U_r = C_1 r + \frac{C_2}{r^2} \quad (3.15)$$

but if the material is homogeneous without any voids or hole then above equation reduces to,

$$U_r = dr \quad (3.16)$$

jump in displacement at the interface is given by the expression,

$$u_r = \lim_{r \rightarrow r^+} U_r - \lim_{r \rightarrow r^-} U_r \quad (3.17)$$

to compute the unknowns we make use of the boundary conditions of traction, continuity and are given by

$$\begin{aligned} \lim_{r \rightarrow r^+} \sigma_r &= f(u_r) \\ \lim_{r \rightarrow r^-} \sigma_r &= f(u_r) \\ \lim_{r \rightarrow \infty} \sigma_r &= \sigma_{rr}^a \end{aligned} \quad (3.18)$$

where f is a scalar function of radial interface displacement jump. making use of above boundary conditions for the unknowns, the jump-in-displacement is comes out to be,

$$\frac{E u_r}{r} = 2(1 - \nu^2) [\sigma - f(u_r)] \quad (3.19)$$

where the matrix and inclusion are assumed to have same elastic properties.

3.2.4 Comparison between analytical and computational results

for, $E = 18.2 \text{ MPa}$, $r = 1\text{mm.}$, $\sigma = 1\text{MPa}$, $\nu = 0.3$

$u_r(\text{computational}) = 0.090909\text{mm}$

$u_r(\text{analytical}) = 0.090909\text{mm}$

Chapter 4

Conclusion and Future Scope

One of the advantages of this technique is that it is possible to determine explicitly the state of stress induced by a dislocation in a range of different geometries in an infinite plane, a half plane, a strip or circular inclusion etc. it is possible to distribute any number of dislocations within the body in question, whilst preserving the boundary condition on the surface of the object, the problem therefore reduces to one of determining the distribution of dislocation which generates tractions, equal and opposite to those produced by external loading.

In chapter-2 the SIF computed for Mode-I and Mode-II cases for a straight and a circular crack matches exactly with the available results given under *Analytical Section*. In case of bi-periodic cracks the computed SIF matches exactly with the available results. In case of bi-periodic cracks the SIF is found to be exactly $P\sqrt{\pi a}$ for large values of parameter α and β , which is the case of a single crack present in an infinite body.

The inclusion problem also gives satisfactory results. The parameter 'K' in the inclusion problem determines the kind of geometry being considered. For $K = 0$ we are characterizing a hole in the body. The opening computed for this case also matches with the opening obtained with the help of ref-[1].

From the previous discussion it is clear that *Distributed Dislocation Technique* can be used to find solution related to fracture mechanics with full accuracy.

Its future scope are,

- Using Distributed Dislocation method one can solve other crack problems involving complicated pattern of cracks in the body. e.g. *Staggered cracks* in a body.
- Inclusion problem can be extended to other type of geometry problems. one can use this method to find the solution for *elliptical* or other type of arbitrary shaped inclusion.

- Inclusion problem can be used to find the effective properties of a material containing voids.
- Inclusion problem can be solved for the case where matrix and inclusion have different elastic properties.
- Non linear cases, where the scalar function of radial displacement jump is not linear dependent on the radial displacement jump, can also be solved.

References

1. A.J.Levy, "The Effective Dilational Response of Fiber-Reinforced Composites With Non-linear Interface", *Journal of Applied Mechanics*, 1996, pp.357-364
2. A.J.Levy, "Separation at a circular Interface under Biaxial Load", *Journal of the Mechanics and Physics of Solids*, Vol 42, 1994, pp.1087-1104
3. D.A.Hills, P.A.Kelly, D.N.Dai, A.M.Korsunsky, "Solution of Crack Problems", *Kluwer Academic Publishers*, 1995.
4. F.Erdogan,G.D.Gupta, "The Numerical Solution of Singular Integral Equations", *Quarterly of Applied Mathematics*, 1972, pp.525-534
5. J.Dundurs and G.P.Sendeckyj, "Edge Dislocation Inside a Circular Inclusion", *J.Mech.Phys.Solids Vol 13*, 1965, pp.141-147
6. J.Dundurs and T.Mura, "Interaction Between an Edge Dislocation and Circular Inclusion" *J.Mech.Phys.Solids vol 12*, 1963, pp.177-188
7. J.Dundurs and T.Mura, *J.Mech.Phys.Solids*, 1974, pp.325
8. L.B.Freund, "Numerical Solution of Singular Integral Equations", 2001, Appendix-A, chapter in *mechanics of thin films (under preparation)*
9. L.B.Freund AND K.S.Kim "Spiral Cracking Around a Strained Cylindrical Inclusion In a Brittle Material and Implication For Vias in Intrigated Circuits", *Mat.Res.Soc.Symp.Proc.Vol.226*, 1991
10. Prashant Kumar "Elements of Fracture Mechanics", *Wheeler Publisher*, 1999
11. V.B.Shenoy, A.F.Schwartzman and L.B.Freund, "Crack Patterns in brittle thin films", *International Journal of Fracture*, 1999
12. Johannes Weertman, "Dislocation Based Fracture Mechanics", *World Scientific publisher*, 1996

133622

133622

Date Slip

The book is to be returned on
the date last stamped.



A133622

TH
ME/2001/M
T 7375
A133622

TH
ME/2001/M
T 7375

A133622

Tripathi, Mukesh Kumar
Solution of Interface Gage
problems using distributed